

Design, Expression, and Functional Analysis of the W123Y BglB Variant via Site-Directed Mutagenesis, Protein Expression, Structural Modeling, and Enzymatic Kinetics

Introduction

β -Glucosidase B (BglB) is an enzyme that catalyzes the hydrolysis of β -glycosidic bonds, producing glucose. This enzyme primarily targets cellobiose and other plant-derived oligosaccharides and is expressed in several different bacterial species. The wild type BglB sequence used in this study is derived from *Paenibacillus polymyxa*, a bacterium that is found worldwide, commonly residing in soil around plant roots. *P. polymyxa* has a symbiotic relationship with plants, promoting growth through nitrogen fixation and enhancing soil health while using plants as a carbon source. As a member of the glycoside hydrolase family, BglB plays an important role in biomass degradation. This function makes β -glucosidases relevant in industrial applications such as biofuel production, food processing, and biotechnology, where efficient carbohydrate breakdown is essential (Bhatia et al., 2002).

Structurally, BglB adopts a barrel structure, commonly referred to as a TIM barrel, consisting of eight β -strands forming an inner barrel surrounded by eight α -helices. This structural motif is highly conserved among glycoside hydrolases and provides a stable framework for enzymatic function. The active site is located at the C-terminal end of the barrel, where loop regions connecting the β -strands and α -helices contribute to substrate binding and catalysis. BglB typically functions as a monomer, and its structural stability is largely derived from the tightly packed core of the barrel. The rigidity and robustness of the TIM barrel scaffold makes it a favorable target for protein engineering, as mutations introduced in the flexible loop regions near the active site can alter binding specificity or heat tolerance without the entire protein collapsing (Wierenga, 2001).

BglB catalyzes glycosidic bond hydrolysis through a double-displacement mechanism involving two glutamate residues, E356 and E167, which function as the nucleophile and acid/base catalyst, respectively. After substrate docking, the acid/base residue protonates the glycosidic oxygen while the nucleophilic residue attacks the anomeric carbon, facilitating cleavage of the bond. As a result, glucose is released, and a covalent glycosyl–enzyme intermediate is formed. Next, E167 acts as a general base, deprotonating a water molecule to generate a reactive hydroxide ion. This ion attacks the anomeric carbon, breaking the covalent bond between the enzyme and substrate and releasing the glucose product while regenerating the active site.

The overall purpose of this study was to design, generate, express, and functionally characterize the W123Y variant of BglB through a three part experimental workflow. First, the mutant plasmid was engineered using site-directed mutagenesis, followed by amplification, purification, and sequence verification. Next, the recombinant W123Y protein was expressed in *E. coli* and purified using affinity chromatography, enabling isolation of the target enzyme. Finally, the structural and functional consequences of the mutation were evaluated using computational modeling and enzyme kinetics assays, allowing comparison of the mutant enzyme to the wild-type.

Through this multi-step approach, this study aims to address how a single amino acid substitution affects enzyme structure, stability, and catalytic activity. This workflow can be replicated to target different amino acid substitutions and proteins, making it versatile for future experiments. Using common biochemical techniques to accomplish protein purification and quantitative enzymatic analysis, the experiment provides insight into the relationship between protein sequence and function. Better understanding this relationship has broad industrial and biomedical applications including enzyme optimization, synthetic protein design, disease prediction, and drug development.

Design and Sequencing of the pET29b-W123Y BglB Variant Using Site-directed Mutagenesis, Plasmid Transformation, and Sanger Sequencing

Materials and Methods

Miniprep

Miniprep buffers were obtained via commercial kit. A stock of DH10B E. coli containing pET29b-BglB (wild type)-6xHis plasmid (WT plasmid) was inoculated in 5 mL of lysogeny broth (LB) with kanamycin, incubating overnight (~16 hrs) at 37°C with 225 rpm shaking. Two aliquots of 2.5 mL of this culture were centrifuged at 4,500 × g for 5 min, discarding supernatant. 250 uL of A1 Resuspension Buffer was added to each of the resulting bacterial pellets. 250 uL of A2 Lysis Buffer was added to each, followed by gentle inversion to mix while minimizing genomic DNA shearing, and incubated at room temperature (~22 °C) for 4 min. 300 uL of A3 Neutralization Buffer was added to each promptly to end incubation, gently inverting until precipitate formation was observed and the samples became colorless. Samples were centrifuged at 16,000 × g for 10 min, and the supernatant was collected and centrifuged again at 16,000 × g for 3 min.

700 uL of each supernatant was added to two NucleoSpin plasmid columns, centrifuging at 16,000 x g for 1 min and discarding flow through. The columns were washed with 500 uL of AW Wash Buffer I followed by 600 uL of A4 Wash Buffer II, centrifuging at 16,000 x g for 1 min and discarding flow through between each step. The columns were dried by centrifuging at 16,000 x g for 4 min and discarding any flow through before 50 uL of AE Elution Buffer was added to each column. The Elution Buffer sat in the columns for 2 min before it was centrifuged at 16,000 x g for 1 min. The two resulting plasmid flow throughs were collected.

Spectrophotometry

Using an Eppendorf BioSpectrometer, Two 2 uL samples of each plasmid flow through was analyzed. 2 uL of Elution Buffer was used to blank the Spectrometer (Parameters: Routine= Nucleic acids, Methods= EXP3-DNA, Cuvette: 1 mm, Unit: ng/μL, Molar Unit: pmol/mL, Factor: 50, Decimal places: 1, A260/280: on, A260/230: on, Autoprint: off), recording absorbance spectra and concentration values.

Gel Electrophoresis

A 1% agarose gel was prepared with 1X Tris-Acetate-EDTA (TAE) buffer and GelStar nucleic acid stain. 3 uL of DNA Ladder as well as two 9 uL plasmid DNA samples (each prepared by mixing 6 uL of plasmid flow through with 1.5 uL 6X DNA Loading Buffer diluted with 1.5 uL molecular grade water (MGW) to yield a final 1X Buffer concentration) were loaded into the gel and electrophoresed at 130 V for 30 min. The gel was then imaged using a Bio-Rad GelDoc Go Imager.

Plasmid Restriction Digest

The following procedure was conducted on both plasmid DNA samples obtained from miniprep. Using the isolated WT plasmid DNA, 4 reactions were performed. 4 uL of plasmid, 2 uL of rCutSmart Buffer, and an appropriate volume of MGW was combined with either 0.5 uL XhoI, NdeI, neither, or both such that 4 solutions were made with total volumes of 20 uL. The 4 reactions were placed into a 37°C water bath for 1 hr.

A 1% agarose gel was prepared as before for gel electrophoresis. 6 uL of DNA Ladder as well as four 24 uL restriction digest samples (each prepared by mixing 20 uL solution with 4 uL 6X DNA Loading Buffer) were loaded into the gel and electrophoresed at 130 V for 30 min. The gel was then imaged using a Bio-Rad GelDoc Go Imager.

Site-directed Mutagenesis

The following procedure was conducted on both plasmid DNA samples obtained from miniprep. Using a forward primer with the W123Y BglB mutation and a back-to-back reverse primer, PCR was performed with the WT plasmid DNA. Plasmid was diluted with MGW for a final concentration of 50 ng/uL and total volume of 20 uL. A Master Mix containing 17.0 uL MGW, 5.0 uL 5X Q5 Reaction Buffer, 0.5 uL of 10 mM dNTPs, and 0.63 uL of both forward and reverse primer (10 uM each) was prepared at 1.1x the required volume. A 25.0 uL PCR reaction was prepared containing 23.75 uL of Master Mix, 1.00 uL of 50 ng/uL plasmid, and 0.25 uL Q5 High-Fidelity DNA Polymerase. A second reaction was prepared as a negative control by replacing the polymerase with 0.25 uL MGW.

The 4 total PCR reactions (both miniprep plasmid samples were prepared) were moved to a thermocycler (Parameters: Initial Denaturation= 98°C, 30 sec; Cycles= 30; Denaturation= 98°C, 10 sec; Annealing= 61°C, 20 sec; Extension= 72°C, 150 sec; Final Extension= 72°C, 4 min; Hold= 4°C, indefinitely). After PCR, samples were stored at -20°C.

A 1% agarose gel was prepared as before for gel electrophoresis. 4 uL of DNA Ladder as well as four 6 uL PCR product samples (each prepared by mixing 5 uL PCR samples with 1 uL 6X DNA Loading Buffer) were loaded into the gel and electrophoresed at 130 V for 30 min. The gel was then imaged using a Bio-Rad GelDoc Go Imager.

KLD Incubation

Using a stock 10X Kinase-Ligase-DpnI (T4 Polynucleotide Kinase, T4 DNA Ligase, and restriction endonuclease DpnI; KLD) Enzyme Mix, the two amplified PCR products were circularized. 1 uL of each amplified PCR product was added to 1 uL MGW, 2.50 uL 2x KLD Reaction Buffer, and 0.50 uL 10X KLD Enzyme Mix, and incubated at room temperature for 20 min.

Bacterial Transformation

Chemically competent DH10B E. coli cells were obtained and used for transformation with KLD-treated plasmid DNA. 5 uL of each of the two KLD reaction products were added to 50 uL aliquots of competent cells. A negative control was prepared using 50 uL of competent cells and no added DNA. After 30 min incubation on ice (~0°C), the three samples were heat shocked at 42°C for 45 sec in a water bath and replaced on ice for 2 min. 250 uL of Super Optimal broth with Catabolite repression (SOC) medium was added to each of the three samples followed by outgrowth at 37°C with shaking at 250 rpm for 1 hr. The samples were

then pelleted by centrifugation at $1,500 \times g$ for 3 min, and ~125 μL of supernatant was discarded. The remaining cells were resuspended in ~150 μL residual SOC medium, and each sample was plated onto kanamycin-selective agar plates (lysogeny broth (LB), 1.5% agar, 50 $\mu\text{g}/\text{mL}$ kanamycin). Plates were incubated at 37°C overnight and stored at 4°C .

Bacterial Inoculation

From each plate exhibiting bacterial growth, a single isolated colony was inoculated into a 14mL round bottom polypropylene tube containing 5 mL LB and 5 mL of 50 $\mu\text{g}/\text{mL}$ kanamycin. This starter culture was incubated at 37°C with 225 rpm shaking overnight. The culture was then centrifuged at $4,000 \times g$ for 10 min at 4°C , discarding supernatant and storing the pellet at -20°C .

Sanger Sequencing

Mutant plasmid DNA was isolated from transformed *DH10B E. coli* using the same miniprep procedure described for wild-type plasmid isolation. As before, plasmid DNA was assessed by spectrometry and 1% agarose gel electrophoresis. Absorbance spectra, concentration values, and gel images were recorded.

The two isolated mutant plasmid samples were sent to a third-party vendor (Genewiz) for Sanger sequencing. 25 μL of each sample was sent (12.5 μL each for T7 promoter forward and T7 terminator reverse primers).

Results

Isolation of pET29b-BglB (wild type)-6xHis Plasmid

A miniprep was performed to isolate WT plasmid from DH10B *E. coli* stock, after which gel electrophoresis and spectrophotometry was performed to determine presence, concentration, and purity. Gel electrophoresis separates DNA by size, and pET29b-BglB (wild type)-6xHis Plasmid is 5,370 bps long. Plasmid DNA generally exists in supercoiled, linear, and nicked forms. Figure 1 shows the imaged gel, with three bands in the 2 elution lanes indicated by red arrows. Relative to the protein ladder, the dark band is approximately 4,900 bps, and the 2 bands above correspond to ~5,400 bps and >7000 bps respectively.

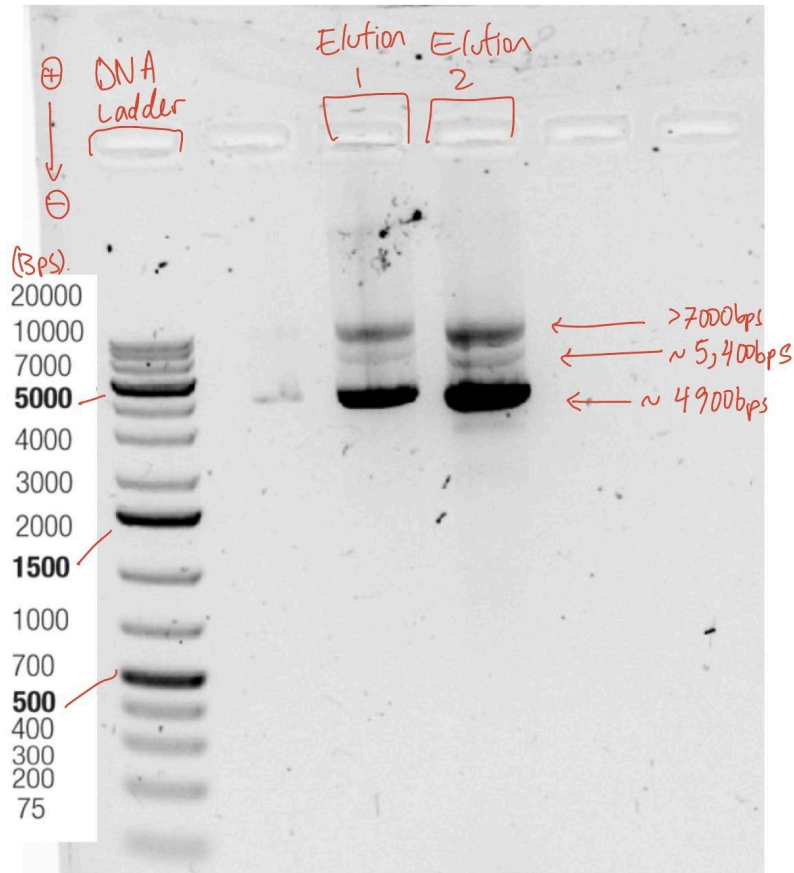


Figure 1, Annotated Post-Miniprep Gel: Miniprep elution separated on a 1% agarose gel. Lane 1: DNA Ladder. Lanes 3-4: Elutions.

The concentration of the isolated WT plasmid can be determined by the equation:
 $[DNA] = (\text{Corrected Absorbance}) * \text{dilution factor} * (500 \text{ ng}/\mu\text{L}) / (1.0 \text{ Absorbance})$.
 The aromatic bases in DNA absorb light at 260 nm most strongly and background solution turbidity can be corrected for by subtracting absorbance at 320 nm. An A260 reading of 1.0 correlates with 500 ng/ μL of pure dsDNA. Purity can be assessed by comparing an A260 value with a protein's maximum absorbance (A260/A280), good-quality DNA will have an A260/A280 ratio of 1.8–2.0.

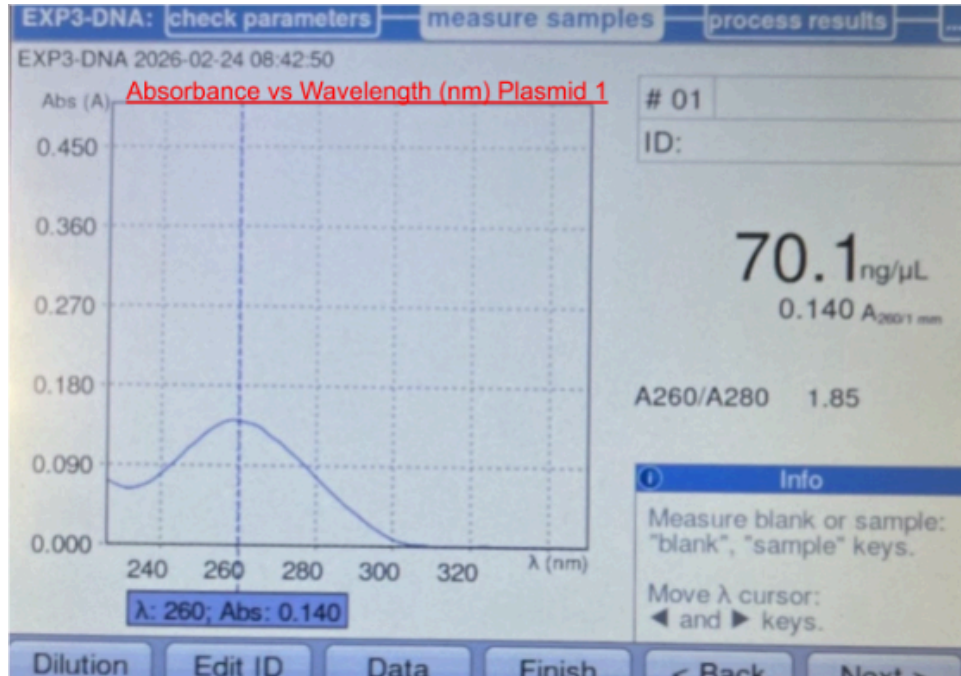


Figure 2, WT Plasmid 1 Absorbance Spectra: The BioSpectrometer absorbance and concentration readings. Measured miniprep elution 1.

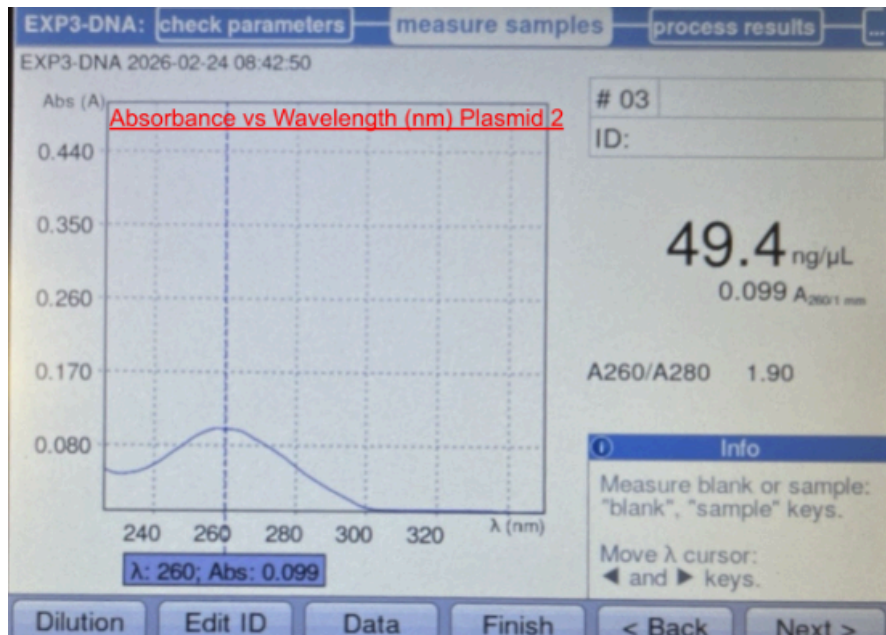


Figure 3, WT Plasmid 2 Absorbance Spectra: The BioSpectrometer absorbance and concentration readings. Measured miniprep elution 2.

Figures 2 and 3 show the absorbance vs wavelength values graphically as well as the calculated concentration and A260/A280 values for the two plasmid samples, labeled Plasmid 1 and 2. Plasmid 1 has a concentration of 70.1 ng/μL and A260/A280 ratio of 1.85. Plasmid 2 has a concentration of 49.4 ng/μL and A260/A280 ratio of 1.90.

Restriction Digestion of the pET29b-BglB (wild type)-6xHis Plasmid

A diagnostic restriction digestion was performed on plasmid 1, testing for the presence of expected structure/restriction sites. Samples containing XhoI, NdeI, neither, or both were electrophoresed. Plasmid 1 and 2 is of the same WT stock, plasmid 1 was assumed to be representative of 2.

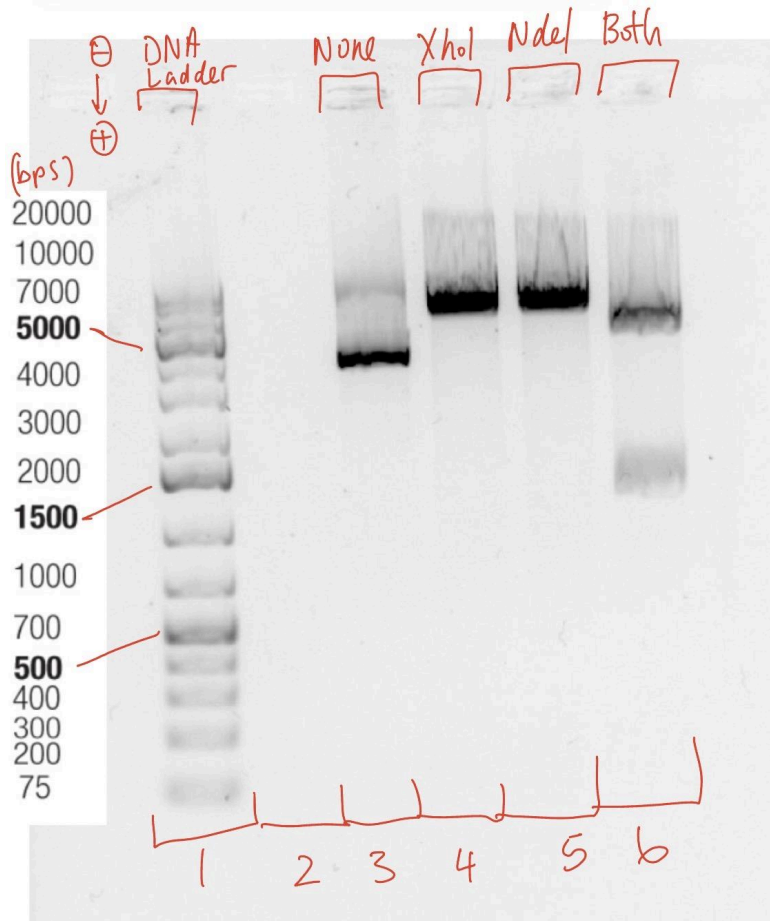


Figure 4, Annotated Restriction Digest Gel: Plasmid 1 restriction digest reaction samples separated on a 1% agarose gel. Lane 1: DNA Ladder. Lane 3: No Enzyme. Lane 4: XhoI Enzyme. Lane 5: NdeI Enzyme. Lane 6: Both XhoI and NdeI Enzyme.

Figure 4 shows the imaged gel, with the 4 samples in lanes 3-6. There are 3 smeared bands in lane 3 corresponding to the 3 bands shown in Figure 1. There is a dark band between 5-7000 bps in lanes 4-5. Lastly there are 2 bands in lane 6 ~5000 bps and ~1400 bps. BglB is 1377 bps long. The smearing shown may have been due to excessive mixing, or due to the large quantity of DNA clumping/dragging during migration.

Site-Directed Mutagenesis of the pET29b-BglB (wild type)-6xHis Plasmid

Site directed mutagenesis (SDM) was performed on WT plasmid 1 and 2 using a mutant forward primer. After SDM was performed, the four samples were loaded onto a 1% agarose gel to analyze if amplification was successful.

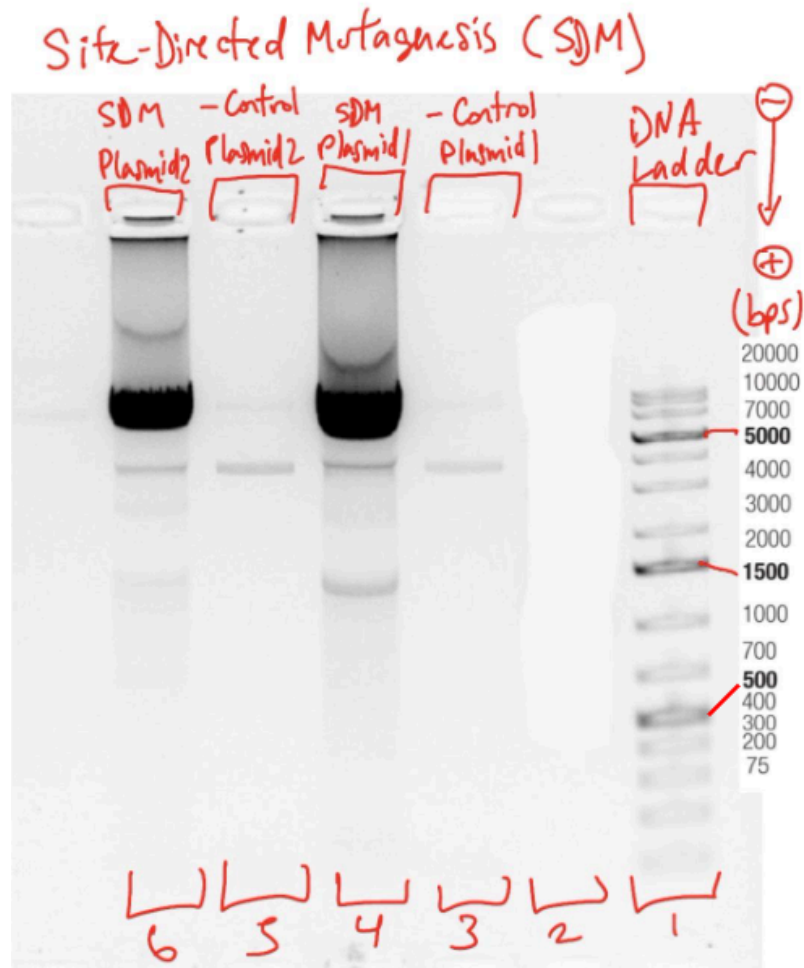


Figure 5, Annotated Post-SDM Gel: Site-directed mutagenesis samples separated on a 1% agarose gel. (Right to Left) Lane 1: DNA Ladder. Lane 3: No polymerase Plasmid 1. Lane 4: post-SDM Plasmid 1. Lane 5: No polymerase Plasmid 2. Lane 6: post-SDM Plasmid 2.

Figure 5 shows the imaged gel, with the 4 samples in lanes 3-6. Another team ran a ladder in lane 2, it is unrelated and edited out for clarity. There is one faint band in lanes 3-6 between 4-5000 bps. In lanes 4 and 6, there is a very dark band between 5000-7000 bps, and additional bands above 7000 bps and below 1500 bps. The smearing shown in lanes 4 and 6 is likely due to the large quantity of DNA clumping/dragging during migration. Based on the very dark band between 5000-7000 bps in lanes 4 and 6, Plasmid 1 and 2 SDM products proceeded to KLD incubation, ligating the linear SDM products and degrading methylated WT plasmid.

Transformation of DH10B E. coli

The 2 KLD-treated plasmids were transformed into chemically competent DH10B E. coli cells. The plasmid conveys bacterial antibiotic resistance, untransformed DH10B E. coli are unable to survive in the presence of kanamycin. After the two transformation samples and negative control sample were heat shocked, they were plated on kanamycin agar plates and incubated.

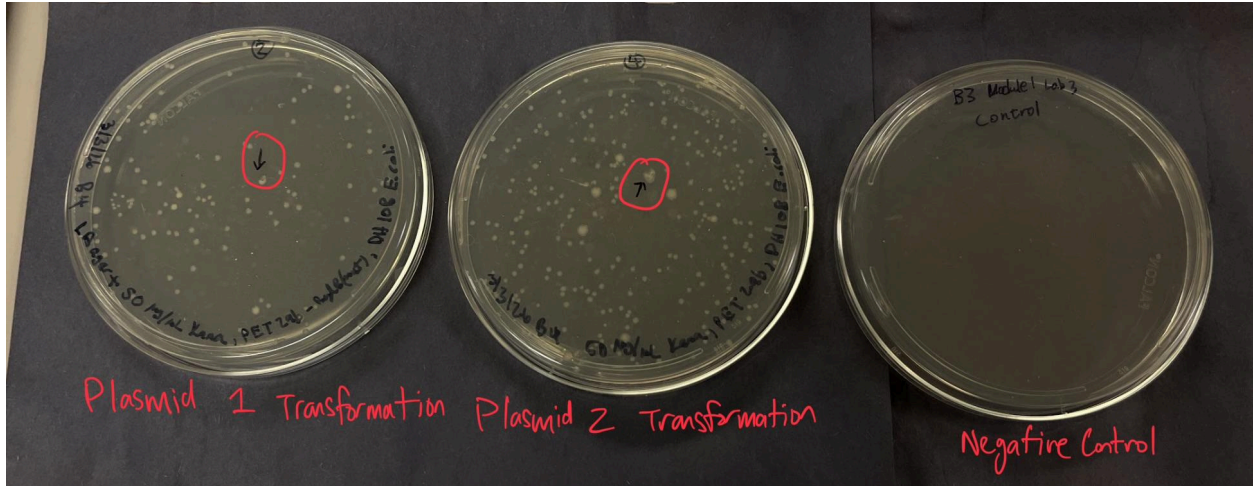


Figure 6, Kanamycin Agar Plates: DH10B cells were plated on LB agar containing 50 ug/mL kanamycin. The left two plates contain the transformation samples, the right contains the negative control sample.

Figure 6 shows many colonies on the two plates with transformed E. coli and no growth on the negative control plate. The circled arrows show the isolated colonies used for inoculation. For the sake of clarity, after inoculation, the plasmids are referred to as mutant plasmid DNA.

Isolation of plasmid DNA from DH10B E. coli

After overnight incubation, the inoculated colonies were processed by miniprep, isolating the mutant plasmid DNA. As before, gel electrophoresis and spectrophotometry was performed to determine presence, concentration, and purity.

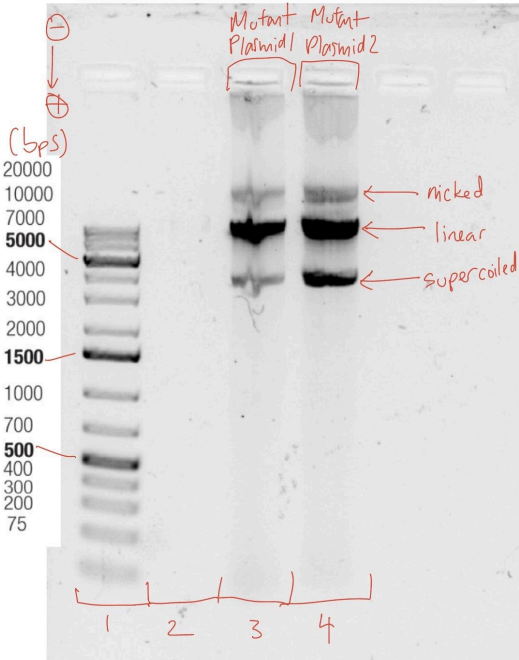


Figure 7, Annotated Post-Miniprep Gel: Miniprep elution of mutant plasmid separated on a 1% agarose gel. Lane 1: DNA Ladder. Lanes 3-4: Elutions.

Figure 7 shows the imaged gel, with three bands in the two elution lanes indicated by red arrows. The three bands correspond with the three bands in Figure 1. The smearing/large size relative to the protein ladder is likely due to the large quantity of DNA clumping during migration. The three bands are labeled as supercoiled, linear, or nicked plasmid based on relative size.

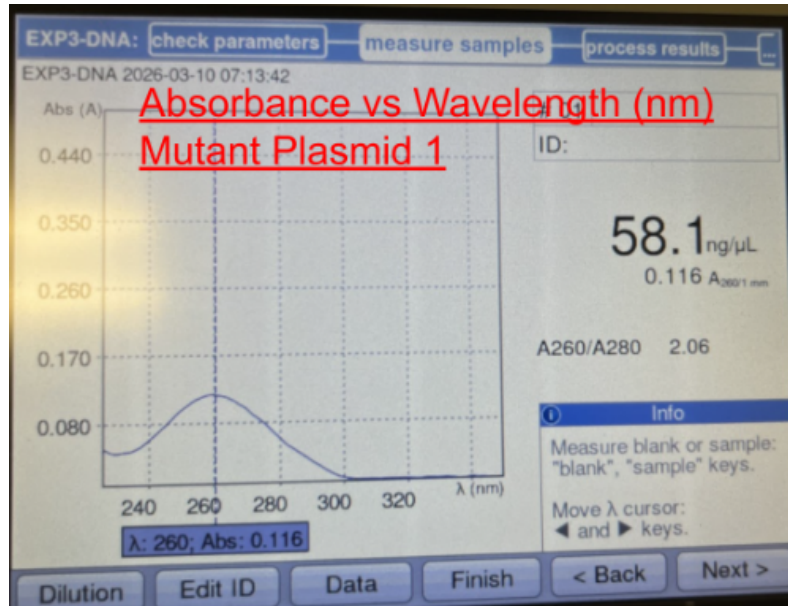


Figure 8, Mutant Plasmid 1 Absorbance Spectra: The BioSpectrometer absorbance and concentration readings. Measured isolated mutant plasmid 1 after miniprep.

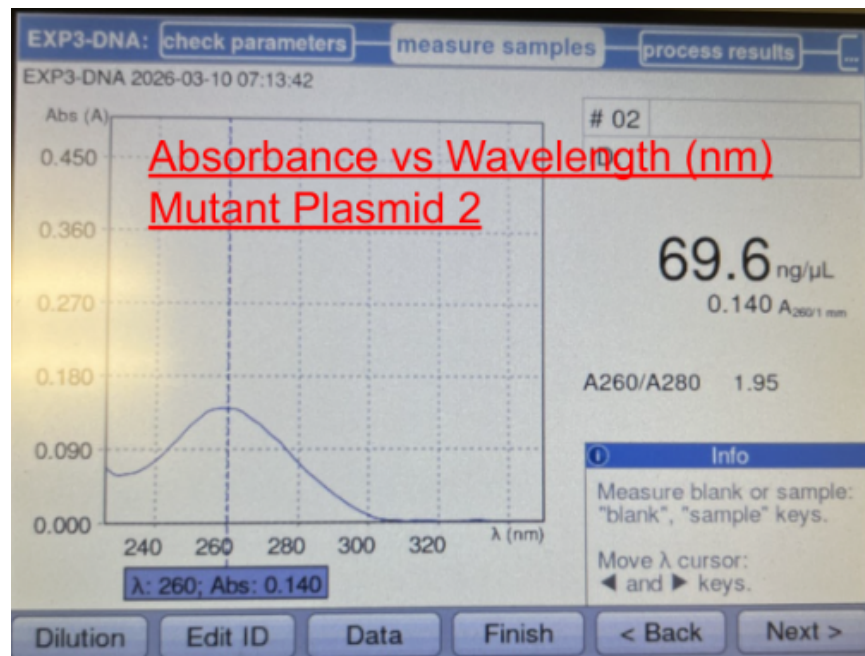


Figure 9, Mutant Plasmid 2 Absorbance Spectra: The BioSpectrometer absorbance and concentration readings. Measured isolated mutant plasmid 2 after miniprep.

Figures 8 and 9 show the absorbance vs wavelength values graphically as well as the calculated concentration and A260/A280 values for the two plasmid samples. Plasmid 1 has a concentration of 58.1 ng/uL and A260/A280 ratio of 2.06. Plasmid 2 has a concentration of 69.6 ng/uL and A260/A280 ratio of 1.95.

Sanger Sequencing Analysis

After isolation, mutant plasmid was sent to a third-party vendor in order to confirm successful W123Y BglB gene mutation in the plasmid. Table 1 shows the forward and reverse sequencing results for mutant plasmids 1 and 2. All four results have QSs above 45 and CRLs above 950. A QS >40 and CRL > 500 is considered good trace results.

Genewiz Sequencing Results			
	Quality Score (QS)	Continuous Read Length (CRL)	Primer
Plasmid 1 T7 Forward	48	986	T7
Plasmid 1 T7 Reverse	48	1001	T7 Term
Plasmid 2 T7 Forward	48	975	T7
Plasmid 2 T7 Reverse	49	988	T7 Term

Table 1, Sequencing Results: The QS and CRL is shown for Plasmid 1 & 2, Forward & Reverse Primers. Used to determine sequencing accuracy.

Sequence alignment was performed using vectorbuilder.com, comparing the sequencing results to the known BglB WT sequence pulled from the Protein Data Bank. Sanger sequencing results are unreliable before 30-40 bps and after 7-900 bps due to the limitations of the assay. As such, only the first ~40-840 bps (adjusting for frame as necessary) of the sequencing results were used for alignment. As BglB is 1377 bps long, there is overlap between the forward and reverse primer results, allowing for complete alignment coverage between the first and last 40 bps.

Sequence Alignment WT BglB vs Engineered W123Y BglB		
DNA alignment based on translated protein sequence.	T7 Promoter Forward Primer (first ~40-840 bps/266 codons)	T7 Terminator Reverse Primer (first ~40-840 bps/266 codons)
Plasmid 1	Sequence 1 length:266 Sequence 2 length:266 Identity: 265/266 (99.62%) Similarity: (100.00%) Gaps: (0.00%)	Sequence 1 length:266 Sequence 2 length:266 Identity: 266/266 (100.00%) Similarity: (100.00%) Gaps: (0.00%)
Plasmid 2	Sequence 1 length:266 Sequence 2 length:266 Identity: 265/266 (99.62%) Similarity: (100.00%) Gaps: (0.00%)	Sequence 1 length:266 Sequence 2 length:265 Identity: 264/266 (99.25%) Similarity: (99.62%) Gaps: 1/266 (0.38%)

Table 2, Sequence Alignment Results: 266 amino acid residues of the reliable sequencing results vs equivalent WT sequence. Used to determine mutation success.

Table 2 shows the adjusted alignment results, reverse primer sequences were reversed and complemented also using vectorbuilder. The reverse primer for plasmid 1 is identical to the WT sequence. The difference between plasmid 2 reverse primer and WT sequence is due to a 3 bp NNN “gap” starting at the 488 bp position as shown by the chromatograph Figure 10. This is due to overlapping signals at this position, 489 bp and 490 bp can be manually assigned G and C which is consistent with WT. This is likely not a mutation, both reverse primers can be considered identical to WT.

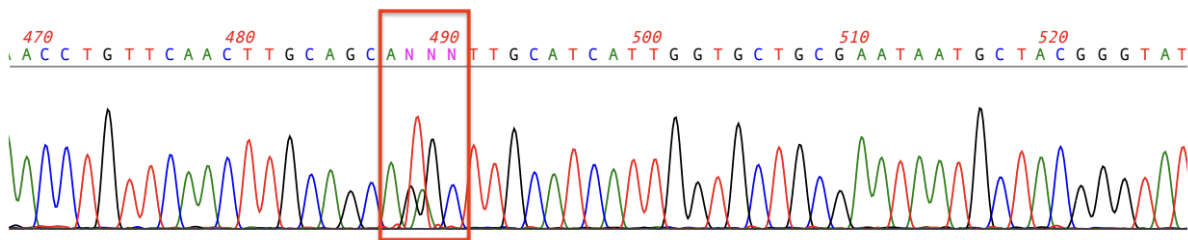
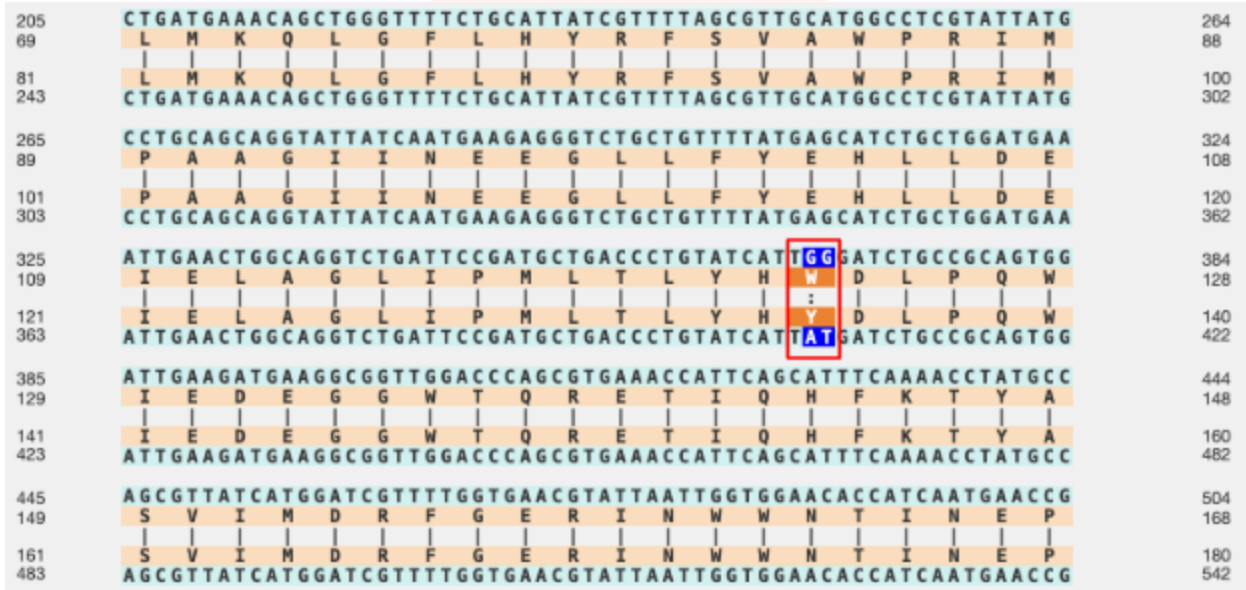


Figure 10, Plasmid 2 Reverse Primer Chromatograph Snippet: 470-525 bp Chromatograph snippet from Sanger Sequencing. The red box highlights unclear signals, particularly at 487 bp.

T7 Forward Primer Plasmid 1



T7 Forward Primer Plasmid 2

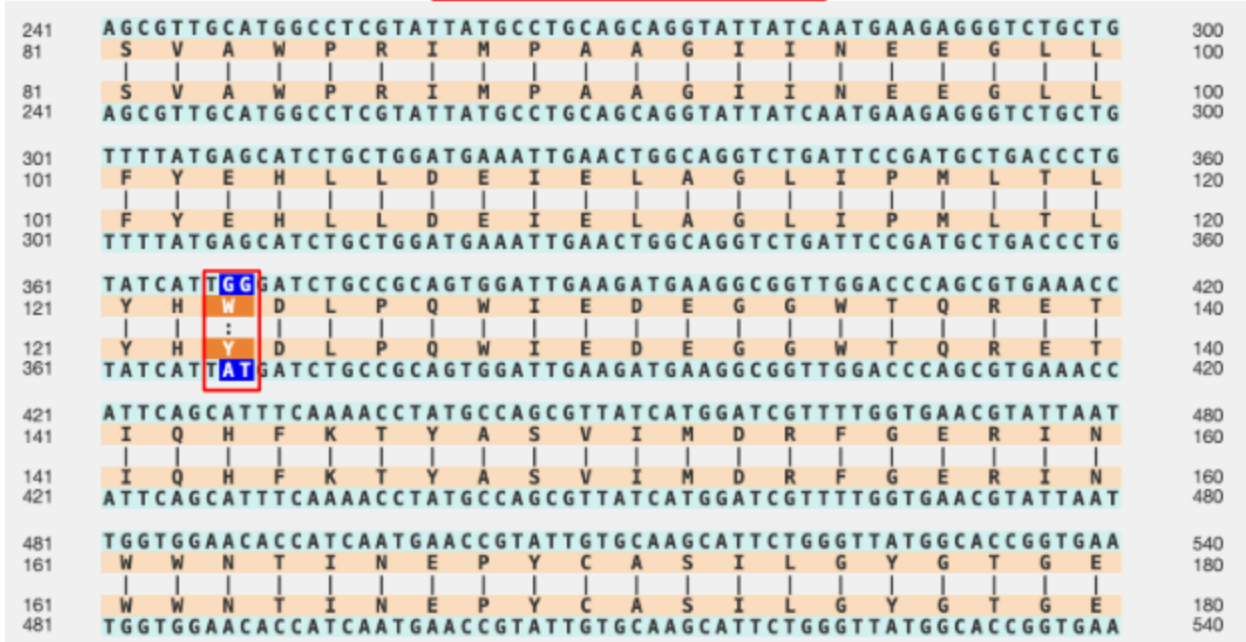


Figure 11, Plasmid 1 & 2 Forward Primer Alignment: Sanger Sequencing results comparing Plasmid 1 & 2 Forward Primer to WT. Within the first 40-840 bps, the only differing bps are boxed in red.

The forward primer for plasmid 1 and 2 both differ from the WT sequence at the same relative position as shown in Figure 11, resulting in a W123Y mutation. The chromatographs of the first ~40-840 bps for all 4 sequences showed clear signal beyond the bps shown in Figure 10.

Expression, Purification, and Detection of Mutant W123Y BglB Protein via Plasmid Transformation, IMAC, SDS-PAGE, Western blot and BCA assays

Materials and Methods

Bacterial Transformation

A stock plasmid (pET29b-BglB(W123Y)-6xHis) and chemically competent BL21(DE3) E. coli cells were obtained. First, the plasmid was diluted to 5 ng/ μ L, two 10 μ L samples of the diluted plasmid were added to separate 50 μ L aliquots of E. coli cells in 1.5 mL microcentrifuge tubes (MCT). Then a third MCT was prepared with 50 μ L E. coli and 10 μ L of molecular grade H₂O as negative control. After 30 min incubation on ice (\sim 0°C), the three samples were heat shocked at 42°C for 45 sec in a water bath and replaced on ice for 2 min. 250 μ L of Super Optimal broth with Catabolite repression (SOC) medium was added to each of the three samples followed by outgrowth at 37°C with shaking at 250 rpm for 1 hr. Approximately 125 μ L of each sample was plated on kanamycin agar plates (lysogeny broth (LB), 1.5% agar, 50 μ g/mL kanamycin), incubated at 37°C overnight (\sim 16 hrs), then stored at 4°C.

Bacterial Inoculation

From each plate exhibiting bacterial growth, a single isolated colony was inoculated into a 14mL round bottom polypropylene tube containing 5 mL LB and 5 mL of 50 μ g/mL kanamycin. This starter culture was incubated at 37°C with 225 rpm shaking overnight.

Bacterial Growth and Protein Induction

An Erlenmeyer flask containing 50 mL LB and 50 μ L of 50 μ g/mL kanamycin was prepared. 500 μ L of this solution was transferred to a cuvette to serve as a blank, and 3 mL of the starter culture was added to the remaining solution within the flask. This expansion culture was loosely covered to prevent contamination and incubated at 37°C with 225 rpm shaking. Cuvettes with 500 μ L of the culture were assessed starting at 0 min with a Genesys 50 UV/Vis spectrophotometer (analysis wavelength to 600 nm, conversion factor to 1.000 \times (108) cells/mL, and instrument factor to 1.000) Measurements were taken every \sim 30 minutes until an OD600 reading of \sim 0.6 was reached. 250 μ L of the expansion culture was centrifuged at 4,000 \times g for 5 min; after Discarding the Supernatant (DS), the resulting pre-induction bacterial pellet was stored at -20°C.

\sim 23 μ L of 1 M IPTG (isopropyl β -D-1-thiogalactopyranoside) was added to the remaining expansion culture for a final concentration of 0.5 mM IPTG to induce protein expression. This flask was shaken at 225 rpm at room temperature (\sim 22°C) overnight. From the culture, 250 μ L was transferred to a MCT and centrifuged at 4,000 \times g for 5 min; after DS the resulting post-induction bacteria pellet was stored at -20°C. The final remaining expansion culture was transferred to a Conical Tube (CT) and centrifuged at 4,000 \times g for 10 min; after DS the resulting final post-induction bacteria pellet was massed and stored at -20°C.

Bacterial Lysis

The cell lysis buffer was prepared: 5 mL of Bacterial-Protein Extraction Reagent (B-PER) per 1 g of bacterial pellet was prepared. Protease inhibitors phenylmethylsulfonyl fluoride (PMSF) and benzamidine hydrochloride (BH) were added to the B-PER at final concentrations of 1 mM PMSF and 1 mM BH, completing the buffer. The final bacterial pellet was dissolved in the lysis buffer and centrifuged at $12,000 \times g$ for 25 minutes at 4°C after rocking for 20 minutes at room temperature. The resulting supernatant contains soluble bacterial components including the target protein and was transferred to a separate CT for purification. The remaining cell lysate pellet was stored at -20°C .

Protein Purification

Equilibration buffer (of 50 mM 4-(2-Hydroxyethyl)piperazine-1-ethanesulfonic acid (HEPES), 150 mM NaCl, at pH = 7.5), Wash buffer (of 50 mM HEPES, 150 mM NaCl, 10 mM 1,3-Diaza-2,4-cyclopentadiene (Imidazole), at pH = 7.5), and Elution buffer (of 50 mM HEPES, 150 mM NaCl, 100 mM Imidazole, at pH = 7.5) was prepared. To target the protein's 6xHis tag, a chromatography column with Ni-NTA (Nickel-Nitrilotriacetic acid) resin was prepared and equilibrated. Affinity chromatography was then carried out using the cell lysate supernatant, collecting the flow-through and 3 rounds of wash and elution samples. The flow-through and wash samples were stored at -20°C .

Dialysis of the three elution samples was conducted in 1X Tris(hydroxymethyl)-aminomethane Buffered Saline (TBS) at pH 7.6 over two days, and replaced with fresh 1X TBS midway through. The samples were then removed and stored at -20°C .

SDS-PAGE

Sodium dodecyl sulfate-polyacrylamide gel electrophoresis (SDS-PAGE) was conducted to resolve sample proteins by size. SDS-PAGE Loading Buffer (containing SDS, glycerol, β -mercaptoethanol, and bromophenol blue) and Running Buffer (of 25 mM Tris, 0.19 M Glycine, 3.47 mM SDS at pH = 8.3) was prepared. Two SDS-PAGE gels (Stacking Layer (4% acrylamide at pH 6.8) Separating Layer (12% acrylamide at pH 8.8)) were cast.

The previously stored 10 samples (Pre/Post-induction, cell lysate, Flow-through, 3x Wash, 3x Elution) were prepped for SDS-PAGE. The pellets were resuspended: Pre/Post-induction with 150 μL diH₂O and cell lysate with 3.5 mL H₂O. Next, 15 μL of each sample was combined with 25 μL 1.6X Loading Buffer for a final concentration of 1X Loading Buffer. The rest of each sample was re-stored at -20°C . After heating at 95°C for 10 minutes, the 10 preparations were run through the two SDS-PAGE gels (100V through the stacking layer and 170V through the separating layer). The first gel was stained with Coomassie, the second gel underwent semi-dry transfer for Western blot.

Coomassie Stain

The first gel was washed in diH₂O to remove excess SDS and then submerged and shaken in Coomassie for 20 min. After staining, the gel was washed in diH₂O over ~46 hrs and imaged via Bio-Rad GelDoc Go.

Semi-dry Transfer and Western Blot

The second gel was placed between 0.45 µm nitrocellulose blotting membrane and blotting paper presoaked in 1X CAPS buffer (10 mM 3-(Cyclohexylamino)-1-propanesulfonic acid at pH 10) and transferred to the membrane via the Bio-Rad Trans-Blot Turbo System at 25V, 1A. The membrane was then stained with Ponceau S to confirm successful transfer and shaken in blocking solution (TBST (1X TBS + 0.1% (v/v) Tween 20) + 5% (weight/volume) nonfat dry milk) for ~46 hrs.

The blocking solution was poured off and the membrane was submerged in 10 mL of 1X TBST. Adding 1 µL of primary antibody (mouse monoclonal anti-6xHis tag) for a 1/10,000 dilution factor, the membrane solution was incubated at room temperature for 45 min on the platform shaker. After washing thrice with 1X TBST, 2 µL of secondary antibody (anti-mouse IgG antibody conjugated to alkaline phosphatase) and 10 mL of 1X TBST was added for a 1/5,000 dilution factor and incubated/washed as before. 5 mL of substrate solution BCIP-NBT [5-bromo-4-chloro-3'-indolophosphate (BCIP)-nitro-blue tetrazolium(NBT)] was added and the membrane was photographed for 5 min, tracking the precipitation.

BCA Assay

The bicinchoninic acid (BCA) assay was conducted to measure protein concentration of the stored 10 samples. Standards A-I of stock 2 mg/mL Bovine serum albumin (BSA) were prepared via a series of serial dilutions (2,000 µg/mL, 1,500 µg/mL, 1000 µg/mL, 750 µg/mL, 500 µg/mL, 250 µg/mL, 125 µg/mL, 25 µg/mL, 0 µg/mL). Dilutions of each sample were prepared using Equilibration Buffer at a 1:4 dilution factor, except for the Post-induction and cell lysate samples (likely have high concentrations) which were prepared at 1:10 dilution factor such that the final volume was 40 µL.

The diluted samples along with the undiluted samples and standards were loaded onto a 96 well microplate. Each sample was loaded in 2 wells of 10 µL such that average absorbance values could be calculated. BCA working solution (15 mL Reagent A (BCA solution) + 300 µL Reagent B (Cu²⁺ solution)) was prepared; 200 µL was added to each used well. The microplate was then incubated for 30 minutes at 37°C. A BioTek Epoch Microplate Spectrophotometer took the absorbance of each well at 562 nm and the absorbance data was recorded and processed, yielding protein concentrations in µg/mL.

Results

BL21(DE3) E. coli Bacterial Transformation and Expansion

The plasmid pET29b-BglB(W123Y)-6xHis conveys bacterial antibiotic resistance, untransformed BL21(DE3) E. coli are unable to survive in the presence of kanamycin. After the two transformation samples and negative control sample were heat shocked, they were plated on kanamycin agar plates and incubated. Figure 1 shows growth on the two plates with transformed E. coli and no growth on the negative control plate. The red arrow shows the isolated colony used for inoculation.

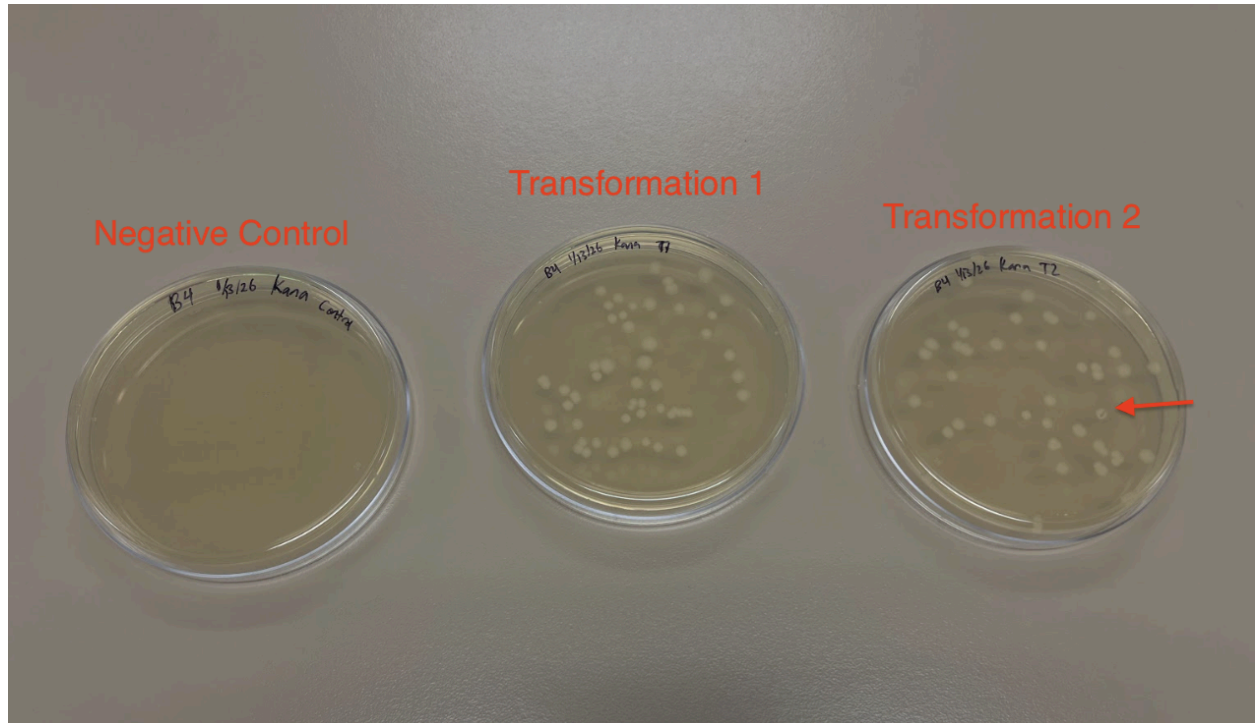


Figure 1, Kanamycin Agar Plates: BL21(DE3) cells were plated on LB agar containing 50 ug/mL kanamycin. The right two plates contain the transformation samples, the left contains the negative control sample.

When expanding the inoculation sample, an OD600 absorbance of ~0.6 indicates the mid-log phase of bacterial growth, when cells are actively dividing and capable of producing large amounts of protein. Incubation was stopped at OD600= 0.592.

Induction of BglB Variant Expression and Protein Purification via Affinity Chromatography

IPTG induces protein expression by binding to the LacI repressor, causing it to dissociate from the lac operator and allowing transcription of the downstream gene under control of the T7 promoter. After induction, the expansion culture was centrifuged and the resulting pre-induction pellet had a mass of 0.53 g. Soluble protein was extracted via lysis buffer and affinity chromatography, allowing for flow through, wash, and elution samples to be run through SDS-PAGE and imaged.

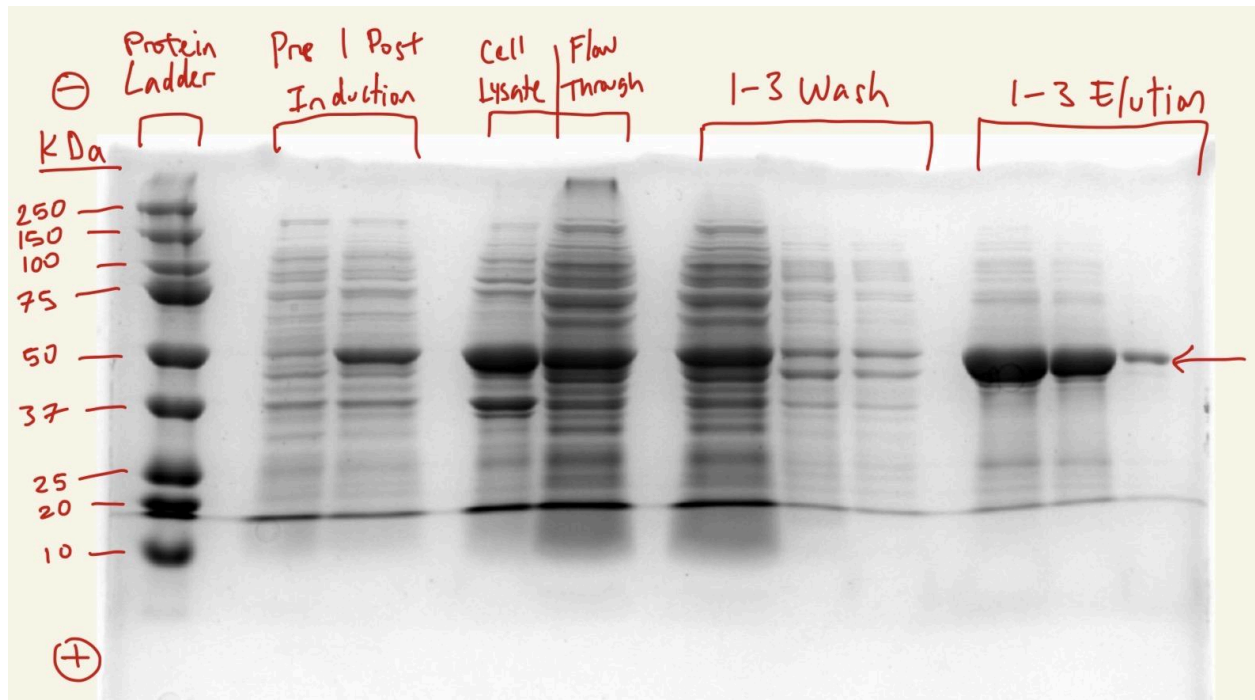


Figure 2, Annotated Coomassie stained SDS-PAGE gel: Proteins were separated on a 12% polyacrylamide gel under denaturing conditions and stained with Coomassie Blue. Lane M: molecular weight ladder (kDa). Lane 1: Protein Ladder. Lane 3-4: Pre and Post-induction samples. Lane 6: cell lysate. Lane 7: Flow-through. Lanes 5-7: Wash samples. Lanes 8-10: Elution samples. Red arrow shows a prominent band at ~50 kDa.

SDS-PAGE separates proteins by size, and BglB is 53-55 kDa. Coomassie Blue allows for clear visualization of all proteins. The Coomassie stained gel in Figure 2 shows a prominent band at ~50 kDa in lanes 4, 6-7, 9-11, and 13-15.

Visual confirmation of BglB

The second gel was transferred to membrane, then the Western blot assay was conducted. Western blot uses antibodies to bind with high specificity to target protein, allowing for accurate protein identification. Alkaline phosphatase attached to antibody converts BCIP-NBT into an insoluble purple precipitate that forms where the enzyme is located on the membrane.

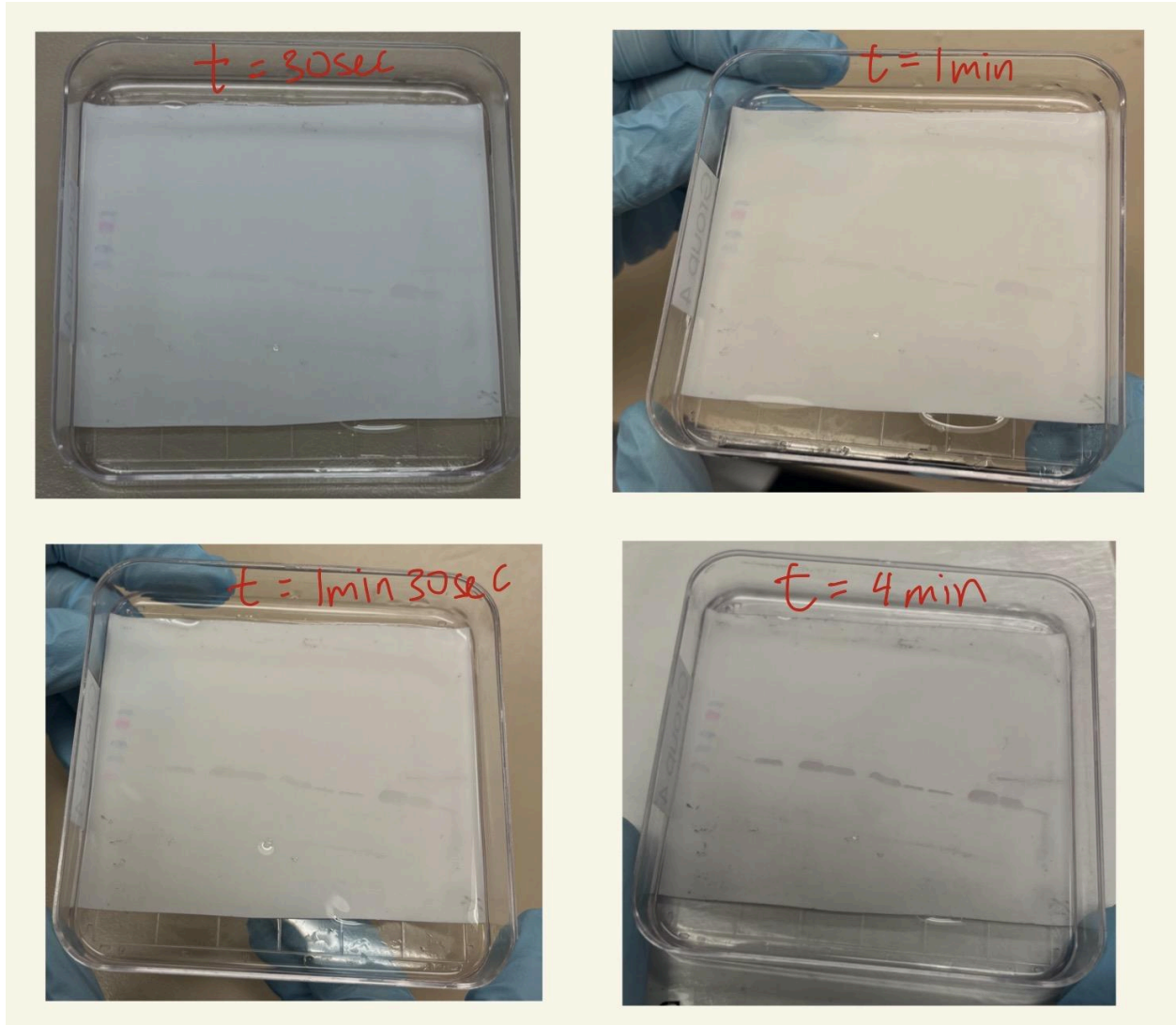


Figure 3, Annotated Western Blot: Proteins on membrane were probed with a primary and secondary antibody followed by detection substrate. Precipitation photographed at 30, 60, 90, and 240 seconds.

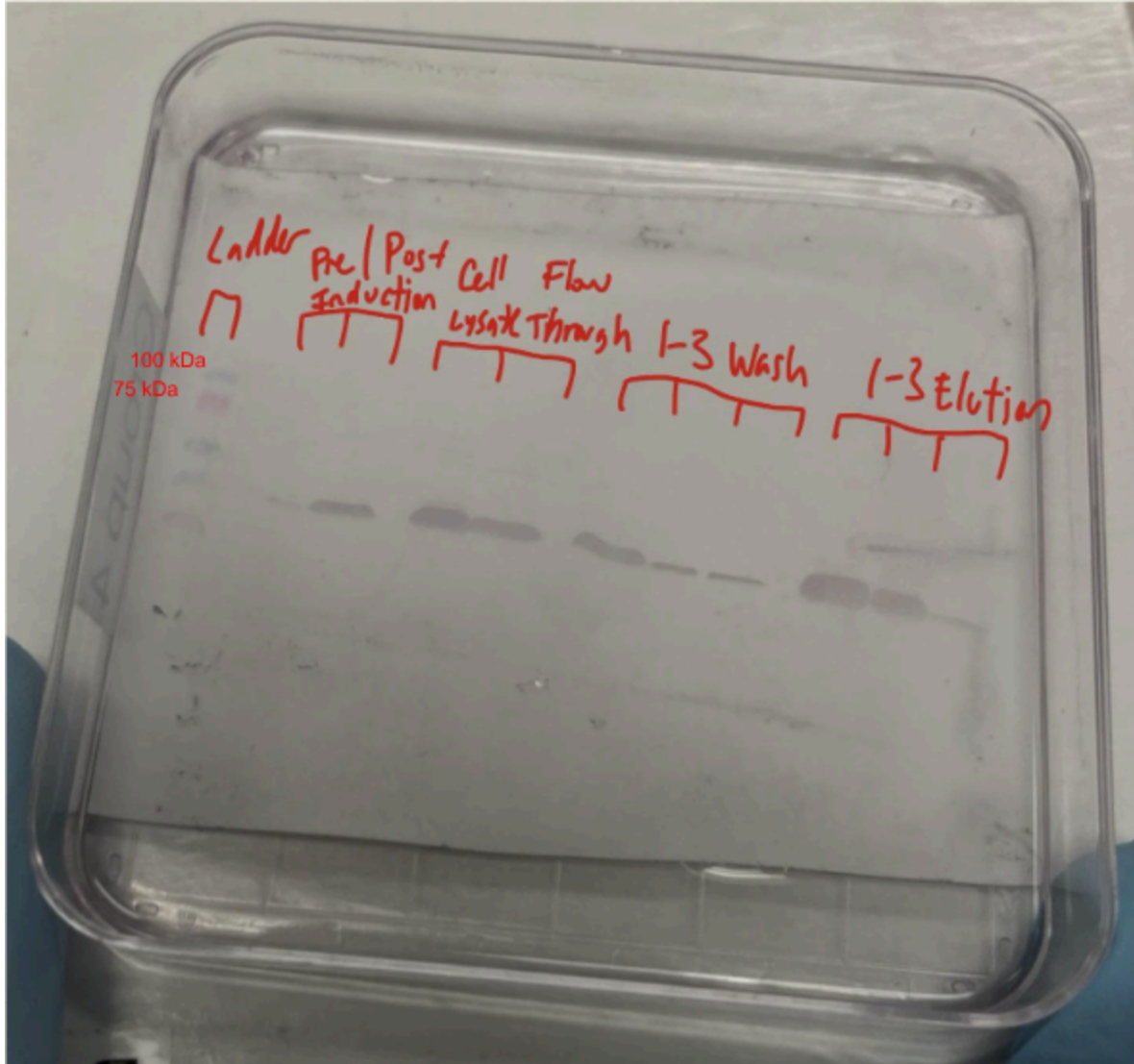


Figure 4, Annotated Western Blot: Membrane after 240 seconds of development where BCIP-NBT precipitate is visible. Lane 1: Protein Ladder. Lane 3-4: Pre and Post-induction samples. Lane 6: cell lysate. Lane 7: Flow-through. Lanes 5-7: Wash samples. Lanes 8-10: Elution samples.

The purple band shown developing in Figure 3 and clearly in 4 corresponds with the ~50 kDa band shown in Figure 2. After 4 minutes band intensity remained the same with no further development.

Quantification of Protein Concentration

After the results of the Western blot, BCA assay was performed to quantify the protein concentration. Proteins reduce Cu^{2+} in the working buffer, and bicinchoninic acid chelates the Cu^+ , generating a purple color proportional to protein concentration.

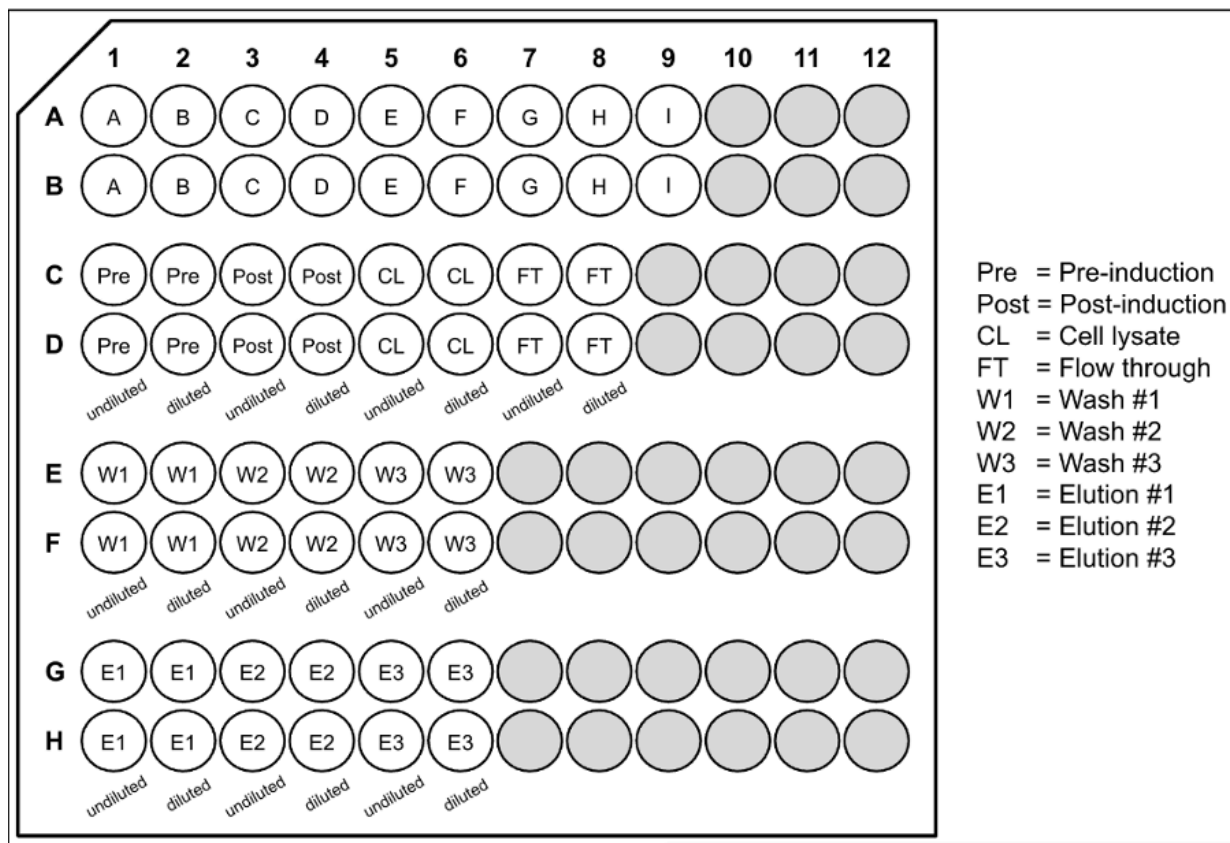


Figure 5, 96 Well Map: A map showing the identity and locations of standards and samples in the 96 well used in BCA assay. Used as a reference for Figures 6, 7.

Plate 2

Matrix Statistics

Data: 562 Edit Matrix

	1	2	3	4	5	6	7	8	9	10	11	12
A	1.069	0.809	0.570	0.415	0.320	0.189	0.137	0.102	0.088	0.047	0.046	0.046
B	1.084	0.757	0.518	0.375	0.308	0.193	0.133	0.097	0.087	0.047	0.047	0.047
C	0.270	0.134	0.503	0.121	1.248	0.292	2.268	0.579	0.047	0.048	0.046	0.047
D	0.332	0.140	1.548	0.123	1.163	0.231	2.152	0.563	0.046	0.046	0.046	0.047
E	1.317	0.324	0.459	0.178	0.312	0.142	0.047	0.047	0.047	0.048	0.047	0.047
F	1.375	0.353	0.504	0.185	0.307	0.127	0.048	0.048	0.049	0.048	0.046	0.047
G	1.138	0.328	0.599	0.185	0.150	0.096	0.048	0.048	0.049	0.048	0.048	0.047
H	1.220	0.343	0.676	0.210	0.158	0.093	0.048	0.046	0.047	0.047	0.048	0.046

Edit Mask Help

Figure 6, BCA Assay Absorbance Readings: The Spectrophotometer absorbance readings. Measured Standards A-I, and Pre/Post-induction, Cell lysate, Flow-through, 3x Wash, and 3x Elution Samples. Sample/Standard locations are given in Figure 5.

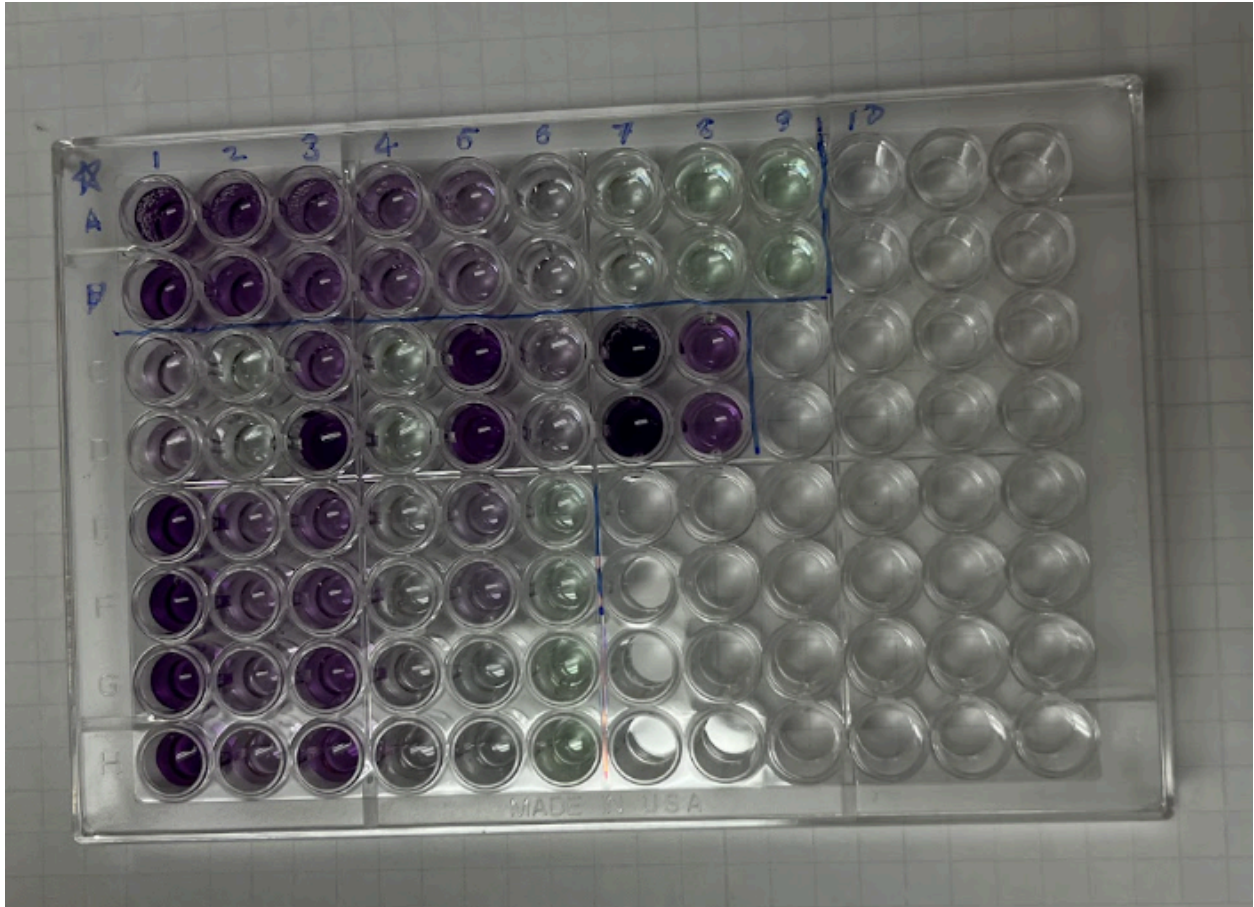


Figure 7, Loaded 96 Well after BCA Assay: The 96 well used for the BCA assay after incubation and absorbance readings. Contains Standards A-I, and Pre/Post-induction, Cell lysate, Flow-through, 3x Wash, and 3x Elution Samples. Sample/Standard locations are given in Figure 5.

Figures 5-7 show the 96 well after incubation and the absorbance data collected. Figure 7 shows the post-induction, cell lysate, flow through, wash 1 and elution 1 visibly dark purple, with a gradient of dark to light purple for standards A-I. Figure 6 corroborates this visual result numerically via the absorbance data.

Corrected Average Absorbance of Standards						
Standard	Protein (µg/mL)	Absorbance Replicate 1	Absorbance Replicate 2	Average Absorbance	Standard Deviation	Absorbance Blank Corrected
A	2000	1.069	1.084	1.0765	0.010606602	0.989
B	1500	0.809	0.757	0.783	0.036769553	0.6955
C	1000	0.57	0.518	0.544	0.036769553	0.4565
D	750	0.415	0.375	0.395	0.028284271	0.3075
E	500	0.32	0.308	0.314	0.008485281	0.2265
F	250	0.189	0.193	0.191	0.002828427	0.1035
G	125	0.137	0.133	0.135	0.002828427	0.0475
H	25	0.102	0.097	0.0995	0.003535534	0.012
I	0	0.088	0.087	0.0875	0.000707107	0

Table 1, Standards: The average absorbance is calculated and displayed alongside the known protein concentration of the standards. Used to generate the trendline.

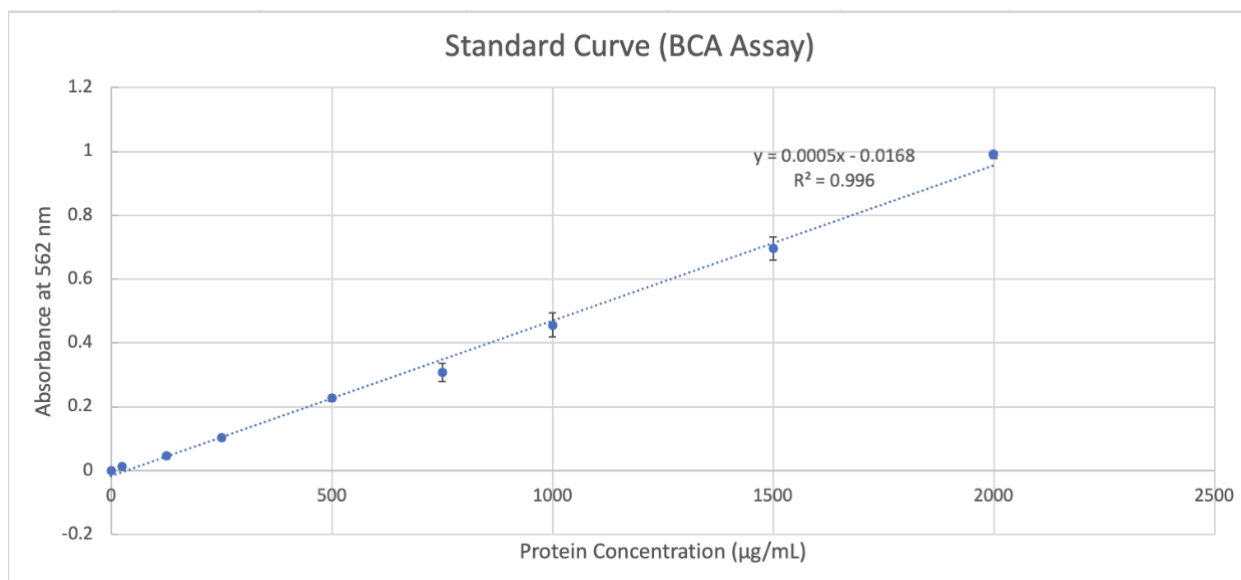


Figure 8, Trendline Graph: The average absorbance graphed against the known protein concentration of the standards. The trendline generated is used to calculate the concentration of the samples.

Table 1 shows the standards A-I's average absorbance, corrected with the blank, and Figure 8 shows those values graphed against their known protein concentrations. The trendline generated is $y = 0.0005x - 0.0168$ with an R^2 value of 0.996. The error bars, as generated with the calculated simple standard deviation values, are small, the trendline is within 7 of the 9 standards' error bars.

1-3 Elution Samples Protein Concentration

Unknown	Abs Replicate 1	Abs Replicate 2	Abs Average	Standard Deviation	Absorbance Blank Corrected	Protein (µg/mL) Initial	Dilution Factor	Protein (µg/mL) Final
E1	1.138	1.22	1.179	0.057982756	1.0915	2216.6	1	2216.6
E1 Diluted	0.328	0.343	0.3355	0.010606602	0.248	529.6	4	2118.4
E2	0.599	0.676	0.6375	0.054447222	0.55	1133.6	1	1133.6
E2 Diluted	0.185	0.21	0.1975	0.01767767	0.11	253.6	4	1014.4
E3	0.15	0.158	0.154	0.005656854	0.0665	166.6	1	166.6
E3 Diluted	0.096	0.093	0.0945	0.00212132	0.007	47.6	4	190.4

Table 2, Concentration of Elution Samples: Used to quantify final yield.

Pre/Post-induction, Cell Lysate, Flow-through, 1-3 Wash Samples Protein Concentration

Unknown	Abs Replicate 1	Abs Replicate 2	Abs Average	Standard Deviation	Absorbance Blank Corrected	Protein (µg/mL) Initial	Dilution Factor	Protein (µg/mL) Final
Pre	0.27	0.332	0.301	0.04384062	0.3885	810.6	1	810.6
Pre Diluted	0.134	0.14	0.137	0.004242641	0.2245	482.6	4	1930.4
Post	0.503	1.548	1.0255	0.738926586	1.113	2259.6	1	2259.6
Post Diluted	0.121	0.123	0.122	0.001414214	0.2095	452.6	10	4526
CL	1.248	1.163	1.2055	0.060104076	1.293	2619.6	1	2619.6
CL Diluted	0.292	0.231	0.2615	0.043133514	0.349	731.6	10	7316
FT	2.268	2.152	2.21	0.082024387	2.2975	4628.6	1	4628.6
FT Diluted	0.579	0.563	0.571	0.011313708	0.6585	1350.6	4	5402.4
W1	1.317	1.375	1.346	0.041012193	1.4335	2900.6	1	2900.6
W1 Diluted	0.324	0.353	0.3385	0.020506097	0.426	885.6	4	3542.4
W2	0.459	0.504	0.4815	0.031819805	0.569	1171.6	1	1171.6
W2 Diluted	0.178	0.185	0.1815	0.004949747	0.269	571.6	4	2286.4
W3	0.312	0.307	0.3095	0.003535534	0.397	827.6	1	827.6
W3 Diluted	0.142	0.127	0.1345	0.010606602	0.222	477.6	4	1910.4

Table 3, Collected Samples Protein Concentrations: Used to quantify yield at each step of the lab.

Using the trendline generated from the standards, the equation $x = (y + 0.0168)/0.0005$ can be used to determine protein concentration of the samples collected over the course of the lab. Tables 2 and 3 show this calculation, with the final protein concentration adjusted for dilution displayed in the far right column. The final protein concentrations match Figure 7, the post-induction, cell lysate, flow through, wash 1 and elution 1 show relatively high protein concentration. These high concentration samples were diluted as the BCA assay is linear at a limited absorbance range, and will give inaccurate concentration values at high concentrations. The diluted final concentration is more accurate for samples with high concentration and large variance in final concentration values. The three elution samples have an average concentration of 1140 µg/mL.

Structural Stability and Enzymatic Activity Analysis of the W123Y BglB Variant Using Computational Modeling, In-Gel Activity Assay, and Kinetic Assays

Materials and Methods

ChimeraX

The 3D atomic coordinates of *Paenibacillus polymyxa* BglB and 4-nitrophenyl β -D-glucopyranoside (pNPG) were pulled from the Protein Data Bank (PDB) and imported into ChimeraX. Using this modeling software, structural motifs, the active site, and the pNPG ligand were visualized as well as the position and orientation of W123Y mutation.

Multiple Sequence Alignment

Pulling *Paenibacillus polymyxa* BglB's sequence from UniProt, a BLAST search was run, allowing for 6 homologous sequences to be pulled. Using these sequences a multiple sequence alignment (MSA) was run via ClustaOmega, allowing for conserved sequences to be visualized.

Foldit

Using PDB files, the wild type BglB structure was loaded into Foldit. Recording the total system energy score, mutations W123Y, N163E, and R243A were individually introduced, noting the change in system energy for each mutation. Additionally, arbitrary mutations A385W, Y414A, and Q369S were each analyzed, noting the change in the system energy.

In-Gel Activity Assay

A 1% agarose gel was prepared for horizontal gel electrophoresis. Three 12 μ L samples of wild-type (WT) BglB were prepared by mixing protein solution with 5X Loading Buffer for a final 1X Buffer concentration (12.5 mM Tris-HCl, pH 6.8; 8% glycerol; 0.002% bromophenol blue). The WT samples contained final BglB concentrations of 0.8 μ g/ μ L, 0.4 μ g/ μ L, and 0.208 μ g/ μ L. Three samples each of the W123Y and R243A BglB variants were prepared at identical volumes and concentrations, yielding nine total samples. These nine samples along with 5 μ L of reference Bovine serum albumin (BSA) were loaded into the gel. Using Native Gel Running Buffer (70 mM Tris-HCl, pH 7.5), gel electrophoresis was performed at 100 volts for 25 min.

5 mM 4-methylumbelliferyl β D-glucopyranoside (4-MUG) substrate was prepared in 0.5 M Tris-HCl at pH 6.8. Ensuring the gel was level, 1 mL of 4-MUG was spread evenly on the gel and incubated at 37°C for 20 min. The gel was then exposed to UV light and imaged using a Bio-Rad GelDoc Go Imager.

The proteins were visualized by Coomassie blue stain. The gel was washed in diH₂O and then submerged and shaken in Coomassie for 20 min. After staining, the gel was washed in diH₂O over ~46 hrs and imaged via Bio-Rad GelDoc Go.

Kinetic Activity Assay

Stock WT BglB at 1.75 μ g/ μ L was quickly assessed for activity by adding 18 μ L of 100 mM 4-nitrophenyl β -D-glucopyranoside (pNPG) stock solution (100 mM pNPG in 100 mM

sodium citrate buffer) to 2 uL of WT BglB. The reactions were incubated at room temperature for 3 min, observing color change. Based on the quick assessment, an approximate dilution was prepared for WT BglB using Assay Buffer (50 mM HEPES (4-(2-Hydroxyethyl)piperazine-1-ethanesulfonic acid), 150 mM NaCl, at pH 6.8). Using a Genesys 50 UV/Vis spectrophotometer (Parameters: λ = 405 nm, Reference λ = — nm, Experiment time= 1 min, Data interval= 0.083 min, Integration time= 0.5 sec) blanked with 100 uL of Assay Buffer, 75 uL of 100 mM pNPG stock was mixed with 25 uL of approximate WT BglB dilution and measured. Adjusting the approximate dilution until reliable absorbance readings (0.1-1.25) was achieved, a 1:50 dilution was chosen for WT BglB.

Using Assay Buffer, a final volume of 400 uL 1:50 WT BglB dilution was prepared. 8 samples of pNPG were prepared via a 3 fold serial dilution (100 mM, 33.33 mM, 11.11 mM, 3.70 mM, 1.23 mM, 0.412 mM, 0.137 mM, 0 mM) with Assay Buffer. 75 uL of each pNPG sample was mixed with 25 uL of WT BglB dilution and measured using the spectrophotometer, recording absorbance over time and ensuring mixing and measuring occurred in quick succession.

This procedure was repeated for previously purified W123Y BglB at 2.12 ug/uL; a 1:50 dilution was determined.

pH and Temperature Optimum Assay

Six pH buffers ranging from pH 3.0 - 8.0 were prepared using 0.2 M Na₂HPO₄ • 2H₂O (pH 8.90) and 0.1 M citric acid (pH 1.95). A 1:50 BglB dilution (both WT and W123Y BglB) was prepared using Assay Buffer (50 mM HEPES, 150 mM NaCl, at pH 7.5). 62.5 uL of each pH buffer and 12.5 uL of each BglB dilution was added in duplicate to a 96-well microplate. An additional blank column using pH 5 buffer and Assay Buffer was included, resulting in 7 x 4 total experimental wells. After allowing the protein to incubate in pH buffer for 10 min, 25 uL of 25 mM pNPG was added to each experimental well, ensuring reactions lasted 2-5 min before 100 uL of stop solution (1 M Na₂CO₃, at pH 12) was added. A BioTek Epoch Microplate Spectrophotometer took the absorbance of each well at 405 nm and the absorbance data was recorded.

Based on the absorbance data, the optimal pH buffer (pH 7) was used to prepare a 1:50 BglB dilution (both WT and W123Y BglB). Six aliquots of each dilution were incubated at 5°C differences (25°C, 30°C, 35°C, 40°C, 45°C, 50°C) for 15 min. The samples were loaded into a 96-well microplate following the reaction setup above, recording enzyme activity as previously described.

Results

Molecular Modeling of BglB Active Site and pNPG Ligand using ChimeraX

The structure of BglB was crystallized by Isorna et. al. and was pulled from the PDB. Figure 1 Left shows the structure of BglB in Chimera X, with residues shown under secondary structures (yellow α -helix, teal β -strands, and white coil). The 8 α -helix and 8 β -strands form the TIM barrel structural motif.

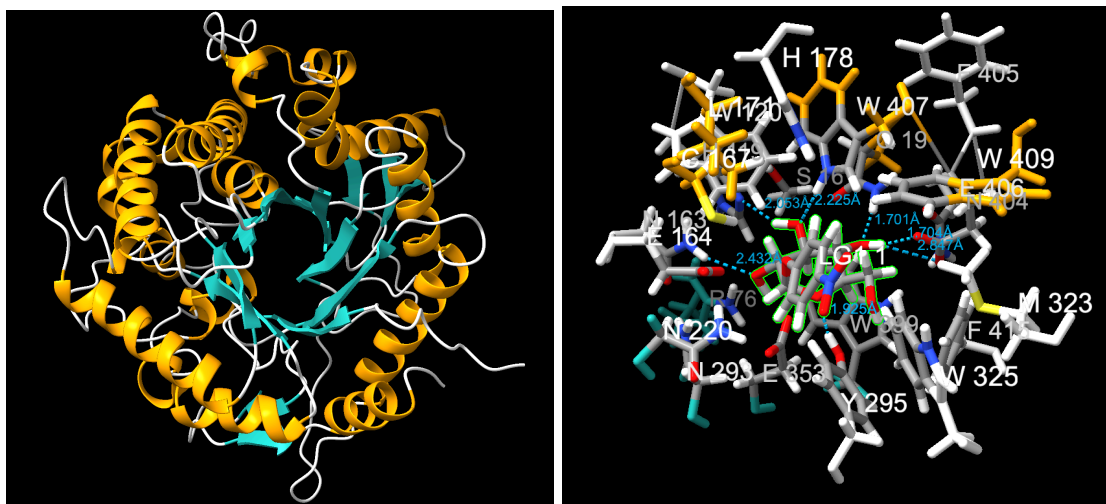


Figure 1 Left, BglB Structure: The structure of BglB in ChimeraX with α -helix in yellow, β -strands in teal, and coil in white.

Figure 1 Right, BglB Active Site Residues: Residues within 5 Å of the LG1 1 ligand. Blue dashed lines denote H bonds between residues and ligand.

Using pNPG (sometimes labeled LG1 1) as the active site ligand, residues within 5 Å were isolated and labeled, as shown in Figure 1 Right. The ligand is highlighted in green, and labeled residues are shifted by 3 as the first 3 residues were not processed in the 3D model. Many surrounding residues have H bond interactions (blue dashed lines) with the ligand, determining its orientation. Figure 2 Left shows catalytic residues E356 and E167 flanking the anomeric carbon (cyan) of the glucose (pink) in pNPG. Figure 2 Right shows the orientation of the W123 residue relative to the active site. W123 (Green) is on a coil within 5 Å of the ligand (the active site residues are shown in pink). The residue's R group extends towards the ligand, 4.039 Å from the anomeric carbon and 2.424 Å at its closest.

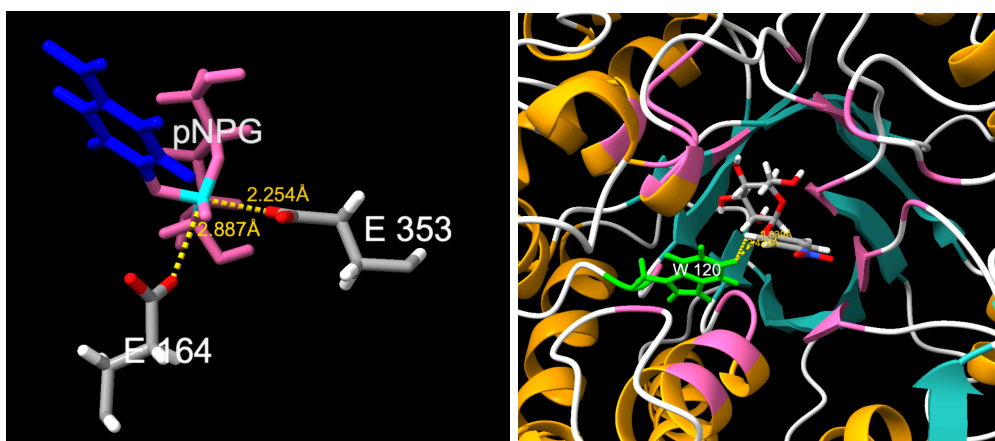


Figure 2 Left, Catalytic Residues and Substrate: Catalytic residues E356 and E167 in ChimeraX flanking the anomeric carbon (cyan) in pNPG.

Figure 2 Right, Residue W123 : Tryptophan 123 in green, yellow dashed lines indicate distance from ligand, pink residues are within 5 Å of the ligand.

Predictive Modeling of BglB Variant Stability using Foldit Standalone

Importing *Paenibacillus polymyxa* BglB structure pulled from PDB into Foldit Standalone, six point mutations were analyzed for stability predictions. The Total System Energy (TSE) of WT BglB was -1089.697 TSE, where a more negative TSE value relates to increased thermodynamic stability. Table 1 shows the predicted TSE for different mutations, calculating the change, $\Delta TSE = \text{Mutant TSE} - \text{WT TSE}$. The conservation of the mutation is noted.

ΔTSE for Mutations Relative to WT			
Mutation	Conservation	Mutant TSE	ΔTSE
W123Y	Conserved	-1069.318	20.379
N163E	Non-conserved	-1083.251	6.446
R243A	Non-conserved	-1087.101	2.596
A385W	Non-conserved	-683.72	405.977
Y414A	Non-conserved	-1080.65	9.047
Q369S	Conserved	-1089.068	0.629

Table 1, ΔTSE for Mutations: Foldit Standalone values for ΔTSE , used to predict stability.

No mutations resulted in a decrease in TSE. Of the variants, A385W resulted in the greatest increase in TSE and Q369S resulted in the smallest increase. ΔTSE values above 5-10 are considered unstable and predict no protein expression.

Assessment of BglB Activity via In-gel Activity Assay

Nine samples of BglB WT and W123Y, R243A BglB variants were run in 1% agarose gel with BSA under native pH 7.5 conditions (folded). Figure 3 shows the gel stained with Coomassie, with protein present in each lane.

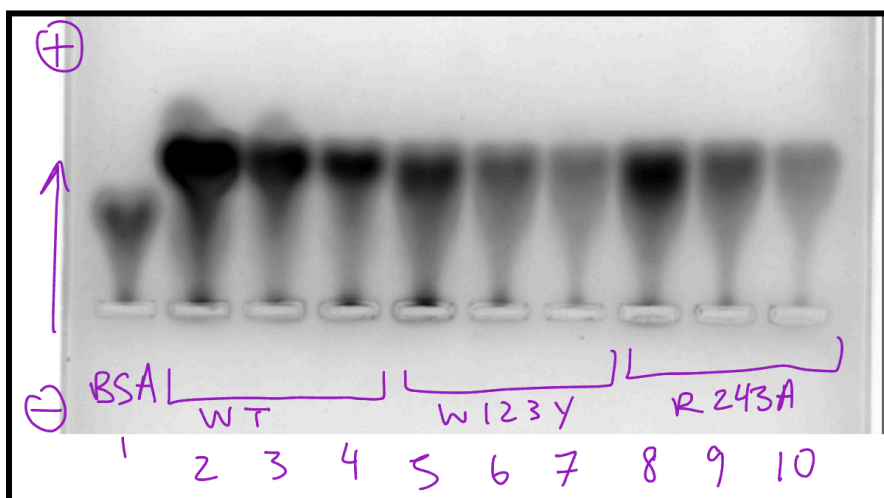


Figure 3, Annotated Coomassie stained gel: Proteins were separated on a 1% agarose gel pH 7.5 conditions and stained with Coomassie Blue. Lane 1: BSA. Lane 2-4: WT BglB. Lane 5-7: W123Y BglB. Lane 8-10: R243A BglB.

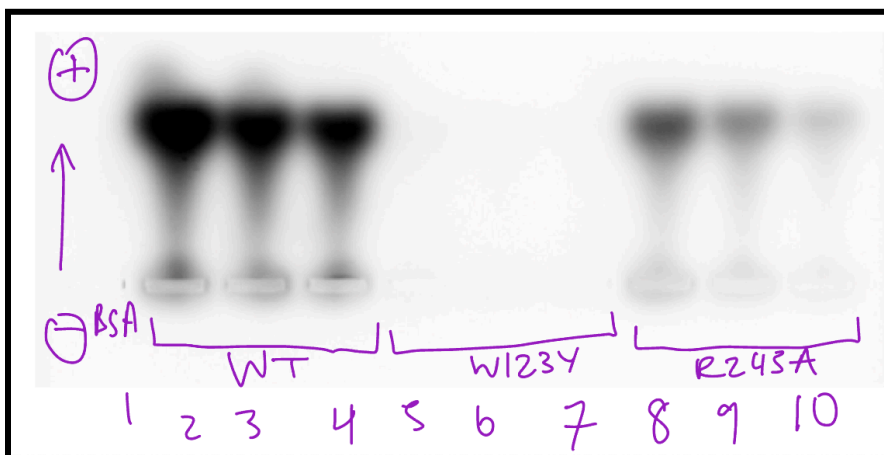


Figure 4, Annotated 4-MUG gel: 4-MUG was spread on proteins in a 1% agarose gel. Lane 1: BSA. Lane 2-4: WT BglB. Lane 5-7: W123Y BglB. Lane 8-10: R243A BglB.

Figure 4 shows the gel imaged after 4-MUG fluorogenic substrate was spread, incubated, and exposed to UV light. Fluorescence is visible in lanes containing WT BglB and more faintly in R243A BglB lanes.

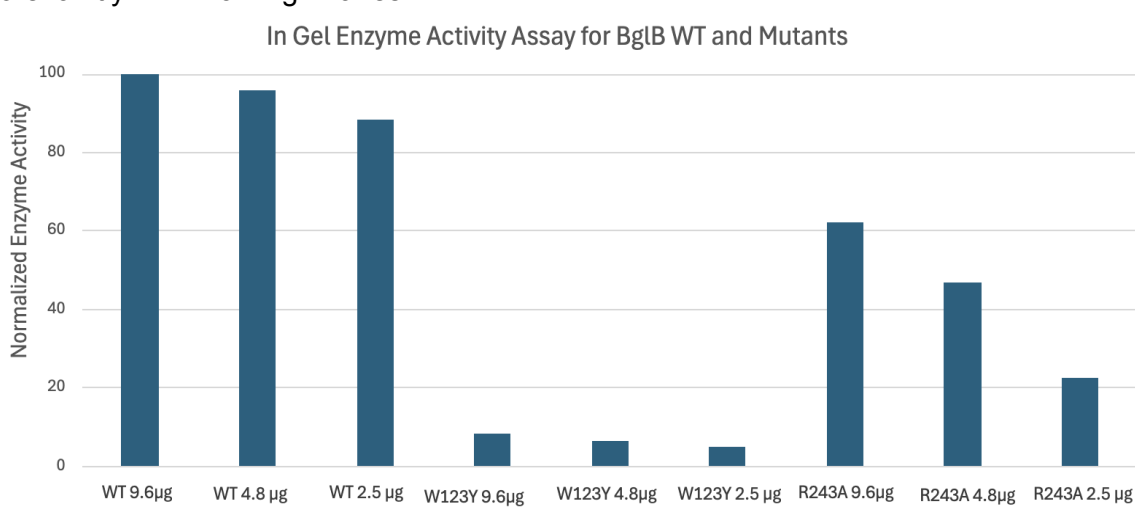


Figure 5, Normalized Enzymatic Activity: Histogram of relative WT and W123Y, R243A variants Enzyme Activity

Figures 3 and 4 were analyzed using ImageJ, using Figure 3 values to normalize Figure 4 data. Figure 5 graphs the relative enzymatic activity for WT BglB vs W123Y, R243A BglB variants. The activity for all WT BglB lanes is well above 80%. The activity for the variants is much lower, peaking at 60% for R243A and under 10% for W123Y, corresponding with Figure 4.

Determination of Kinetic Constants for BglB via Kinetic Activity Assay

A 1:50 dilution of both WT and W123Y BglB was reacted with varying concentrations of pNPG, recording absorbance over time. This measurement was analyzed by converting it to a reaction initial velocity (V_0 in $\mu\text{M}/\text{min}$) using the Beer-Lambert law ($A = \epsilon cl$; where A = absorbance/time, $c = V_0$, ϵ is molar absorptivity of pNPG = $11,700 \text{ M}^{-1} \text{ cm}^{-1}$, and l is pathlength = 1 cm). Figure 6 shows a sample V_0 calculation for WT reaction C. Table 2 shows calculated V_0 values for BglB, correcting for the 0 mM pNPG sample and any non-linear absorbance rates (plateau). Both WT (under blue) and W123Y (under purple) values are shown, with the V_0 values conditionally formatted for magnitude.

Ex Rxn C

$$A = 0.8872 \Delta \text{Abs}_{405\text{nm}}/\text{min} \quad \epsilon = 11700 \text{ M}^{-1} \text{ cm}^{-1} \quad l = 1 \text{ cm}$$

$$V_0 = C = \frac{A}{\epsilon l} = \frac{0.8872 \left(\frac{\Delta \text{Abs}_{405\text{nm}}}{\text{min}} \right)}{11700 \text{ M}^{-1} \text{ cm}^{-1} \cdot 1 \text{ cm}} = 7.58 \cdot 10^{-5} \frac{\text{M}}{\text{min}} \cdot \frac{10^6 \mu\text{M}}{1 \text{ M}} = \underline{75.83 \mu\text{M}/\text{min}}$$

Figure 6, V_0 Sample Calculation: The Beer-Lambert Law was used to calculate V_0 from a measured ΔABS (405nm)/min Value.

Calculated V_0 from ΔABS (405nm)/min Values									
WT					W123Y				
Reaction	ΔABS (405nm)/min	Blank Corrected	V_0 ($\mu\text{M}/\text{min}$)	Final mM [pNPG]	ΔAbs (405)/min	Blank Corrected	V_0 ($\mu\text{M}/\text{min}$)	Final mM [pNPG]	
A	0.226	0.2262	19.3333333	75	0.0121	0.012	1.02564103	75	
B	0.536	0.5362	45.8290598	25	0.0441	0.044	3.76068376	25	
C	0.887	0.8872	75.8290598	8.33	0.0499	0.0498	4.25641026	8.33	
D	0.7894	0.7896	67.4871795	2.78	0.0172	0.0171	1.46153846	2.78	
E	0.4237	0.4239	36.2307692	0.93	0.0065	0.0064	0.54700855	0.93	
F	0.1501	0.1503	12.8461538	0.31	-0.0037	-0.0038	-0.3247863	0.31	
G	0.0613	0.0615	5.25641026	0.1	0.0002	0.0001	0.00854701	0.1	
H	-0.0002	0			0.0001	0			

Table 2, Calculated V_0 Values: Beer-Lambert Law is used to calculate V_0 , data under blue corresponds to WT and purple for W123Y. Used to generate Michaelis-Menten Curves.

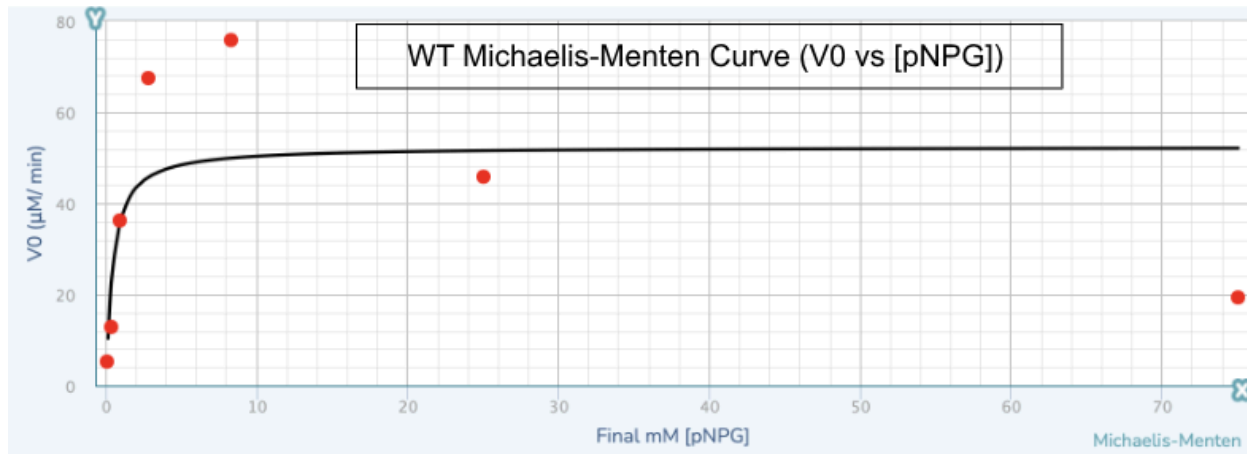


Figure 7, WT Michaelis-Menten Curve: V_0 graphed against [pNPG] and fit to Michaelis-Menten Equation.

Figure 7 shows WT BglB's V_0 graphed against final pNPG concentration and fit to the Michaelis-Menten Equation ($V_0 = V_{max} \frac{[pNPG]}{K_m + [pNPG]}$) using mycurvefit.com. Due to high pNPG availability in reactions A and B, the initial absorbance rates were difficult to accurately capture. Excluding reactions A and B, Figures 8 and 9 show the adjusted Michaelis-Menten Curve for WT and W123Y BglB, yielding $V_{max} = 91.987 \text{ uM/min}$, $K_m = 1.37 \text{ mM}$ for WT and $V_{max} = 0.803 \text{ uM/min}$, $K_m = -0.52 \text{ mM}$ for W123Y. The curve approximation for W123Y is atypical and not a good fit as the V_0 values are very small.

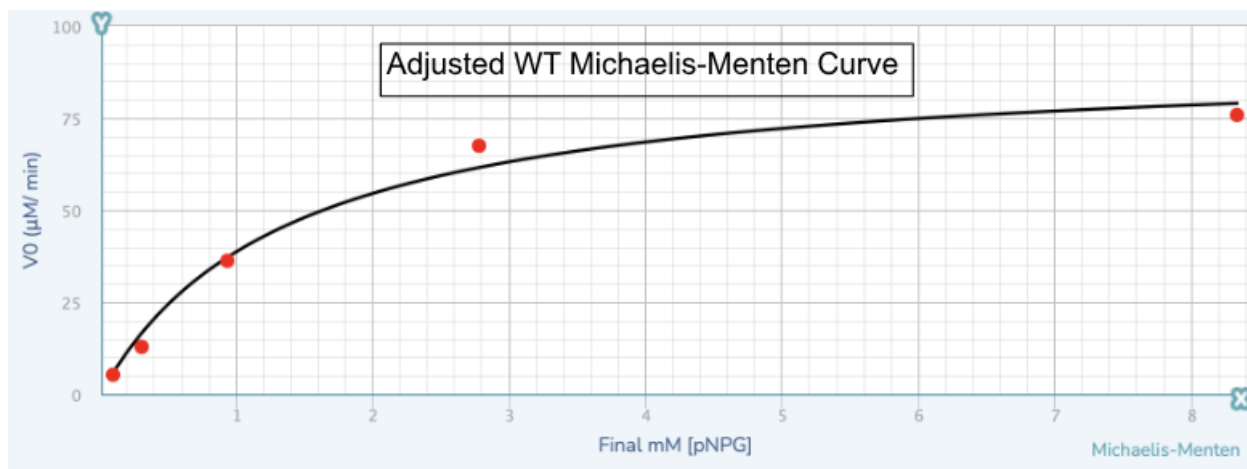


Figure 8, Adjusted WT Michaelis-Menten Curve: V_0 graphed against [pNPG] for reactions C-G and fit to Michaelis-Menten Equation.

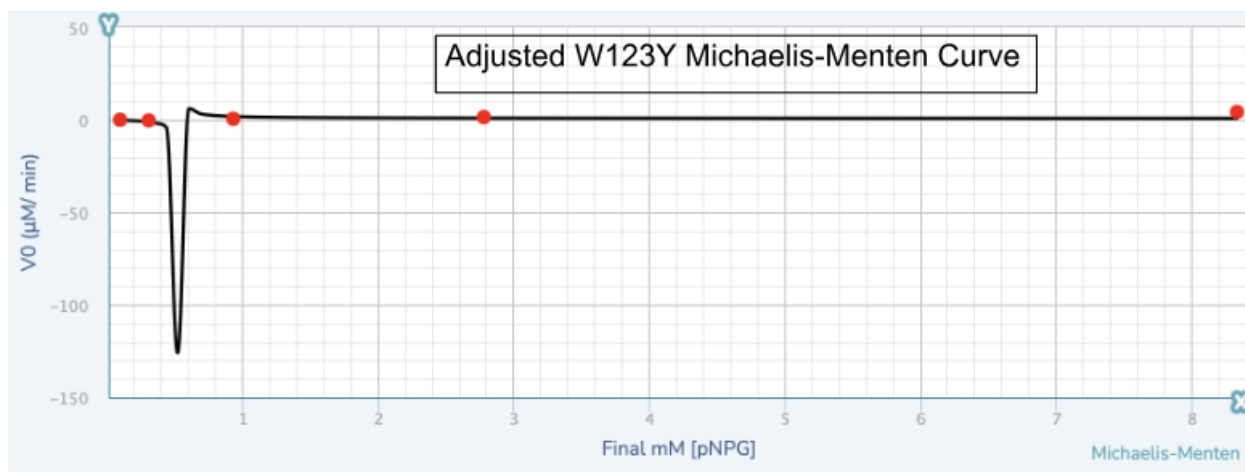


Figure 9, Adjusted W123Y Michaelis-Menten Curve: V_0 graphed against [pNPG] for reactions C-G and fit to Michaelis- Menten Equation.

The turnover number, K_{cat} ($K_{cat} = V_{max}/ [BglB]_{total}$) can be used to determine catalytic efficiency (CE) of an enzyme ($CE = K_{cat}/K_m$). Table 3 shows the $[BglB]_{total}$ ($[BglB]_{final}$) values calculated, using the initial WT and W123Y BglB concentrations ($\mu\text{g}/\mu\text{L}$), BglB’s molar mass (52,782 g/mol) and the dilution factor. Using these values, Table 4 shows the calculated K_{cat} and CE of the WT and W123Y BglB enzyme.

[BglB] _{final} Determination			
Protein	[BglB] _{stock} (μM)	Final Dilution Factor for Assay	[BglB] _{final} (μM)
WT	33.1552423	1:50	0.663104846
W123Y	39.4073737	1:50	0.788147475

Table 3, Calculated [BglB]_{final}: Used to calculate K_{cat} .

Michaelis-Menten Plot				
Protein	K_m (mM)	V_{max} ($\mu\text{M}/\text{min}$)	k_{cat} (1/min)	Catalytic efficiency (1/ mM*min)
BglB WT	1.37	91.987	138.7216525	101.2566806
W123Y	-0.52	0.803	1.018844855	-1.959317029

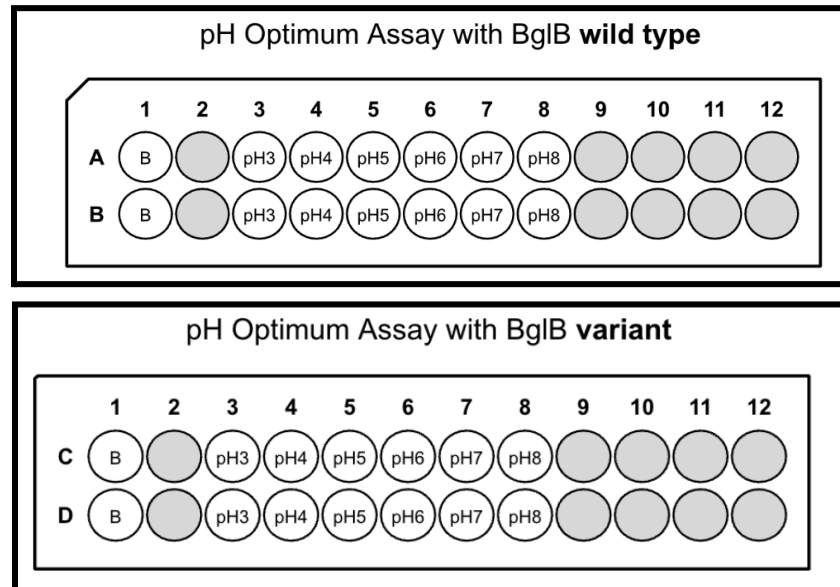
Table 4, Calculated K_{cat} and CE Values: Used to quantify enzyme activity.

The CE, K_{cat} , V_{max} , and K_m constants for WT BglB are much larger than that of the W123Y variant. The CE and K_{cat} values for W123Y are very low, the negative CE value is due to the K_m value determined from the atypical Adjusted W123Y Michaelis-Menten Curve. The change in absorbance over time for the variant was very small for all reactions, as a result small perturbations had a large impact on calculations.

Determination of pH and Temperature Optimum for BglB via Activity Assay

A set volume of WT and W123Y BglB was reacted with pNPG substrate in 6 different pH buffers (pH3.0-pH8.0), allowing reactions to continue until a 2-5 min endpoint.

Figure 10, 96 Well Map: A map showing the locations of samples in the 96 well used in the pH optimum Assay. B is for blank. Used as a reference for Figure 11.



This endpoint assay was done in a 96 well plate as shown by the map Figure 10, the corresponding absorbance readings are shown in Figure 11. The conditional formatting in the spectrophotometer output indicates high absorbance.

	1	2	3	4	5	6	7	8	9	10	11	12
A	0.071	0.055	0.072	0.072	1.606	1.593	1.692	0.922	0.055	0.059	0.054	0.055
B	0.073	0.055	0.070	0.071	1.300	1.540	1.724	1.075	0.056	0.056	0.054	0.056
C	0.072	0.055	0.077	0.070	0.149	0.126	0.082	0.077	0.055	0.056	0.055	0.056
D	0.074	0.056	0.066	0.072	0.050	0.088	0.102	0.073	0.055	0.055	0.055	0.055

Figure 11, pH Optimum Absorbance Readings: The Spectrophotometer absorbance readings. Measured enzyme reactions in six pH buffers.

Figure 11 shows pH buffer 7 had the highest significant absorbance, and was used to conduct the temperature optimum assay. Using a similar reaction setup as pH optimum, set volumes of WT and W123Y BglB was incubated at 6 different temperatures (25°C-60°C) and then reacted with pNPG substrate, allowing reactions to continue until a 2-5 min endpoint. The 96 well map is shown in Figure 12, the corresponding absorbance readings are shown in Figure 13.

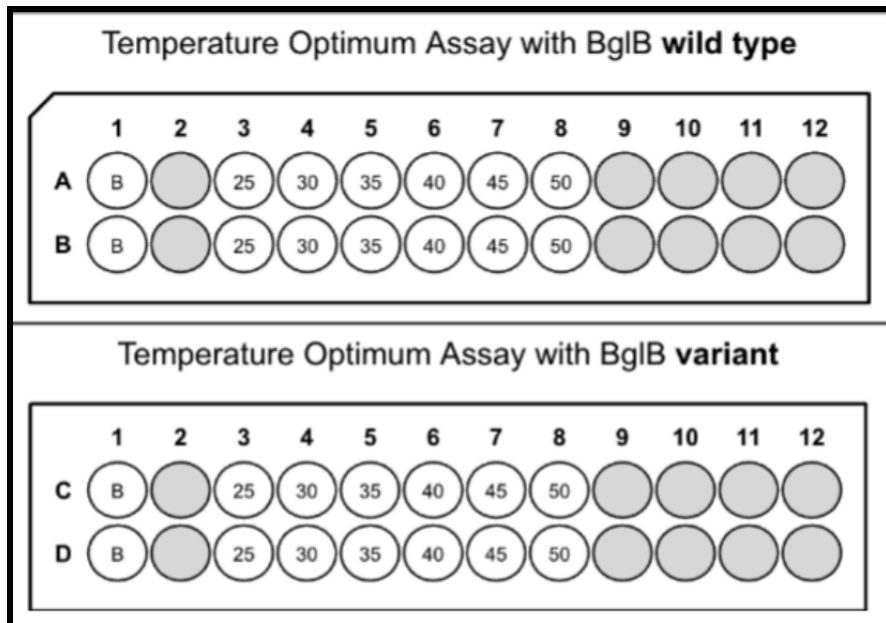


Figure 12, 96 Well Map: A map showing the locations of samples in the 96 well used in the pH optimum Assay. B is for blank. Used as a reference for Figure 13.

	1	2	3	4	5	6	7	8	9	10	11	12
A	0.072	0.066	1.714	1.946	1.871	1.135	0.100	0.066	0.055	0.055	0.055	0.057
B	0.069	0.058	1.901	1.829	2.052	1.273	0.093	0.066	0.055	0.055	0.055	0.057
C	0.063	0.055	0.096	0.092	0.075	0.064	0.063	0.069	0.056	0.056	0.055	0.091
D	0.066	0.056	0.104	0.099	0.084	0.082	0.065	0.063	0.056	0.056	0.056	0.056

Figure 13, Temperature Optimum Absorbance Readings: The Spectrophotometer absorbance readings. Measured enzyme reactions after incubation at 6 different temperatures.

For both the Temperature and pH optimum absorbance data, relative enzyme activity % was calculated by taking the duplicate average, correcting for blank, and calculating the concentration of pNPG produced using the Beer-Lambert Law, before dividing all values by the highest concentration. Figures 14-17 show this relative enzyme activity % for WT and W123Y BglB plotted against pH or temperature, respectively, using mycurvefit.com to fit to a Gaussian Curve.

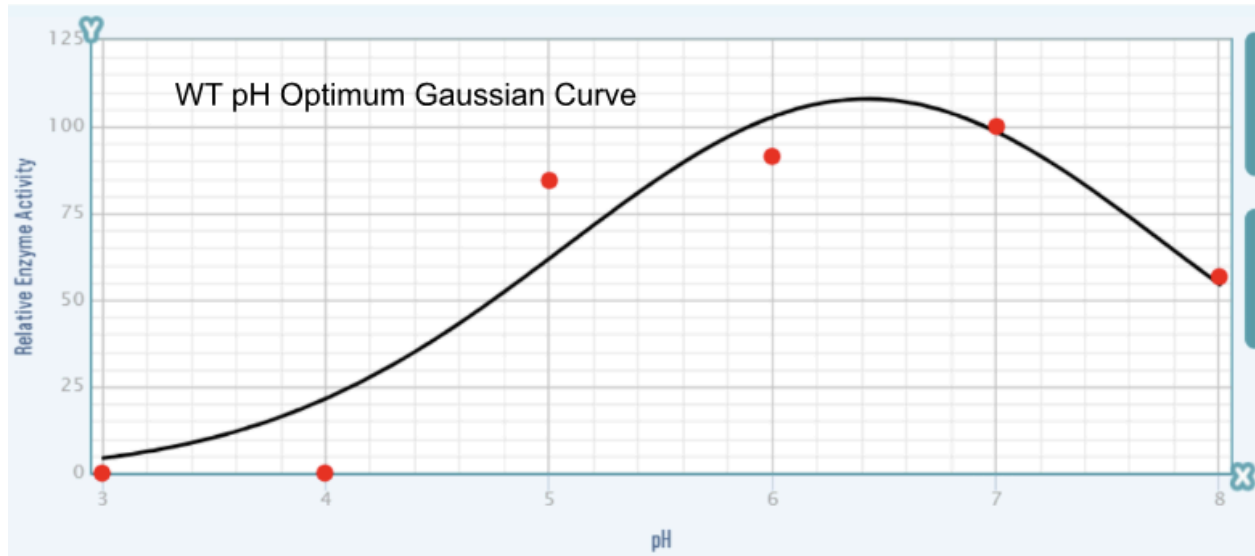


Figure 14, WT pH Optimum Gaussian Curve: Relative Enzyme Activity graphed against pH. Used to determine the optimal pH.

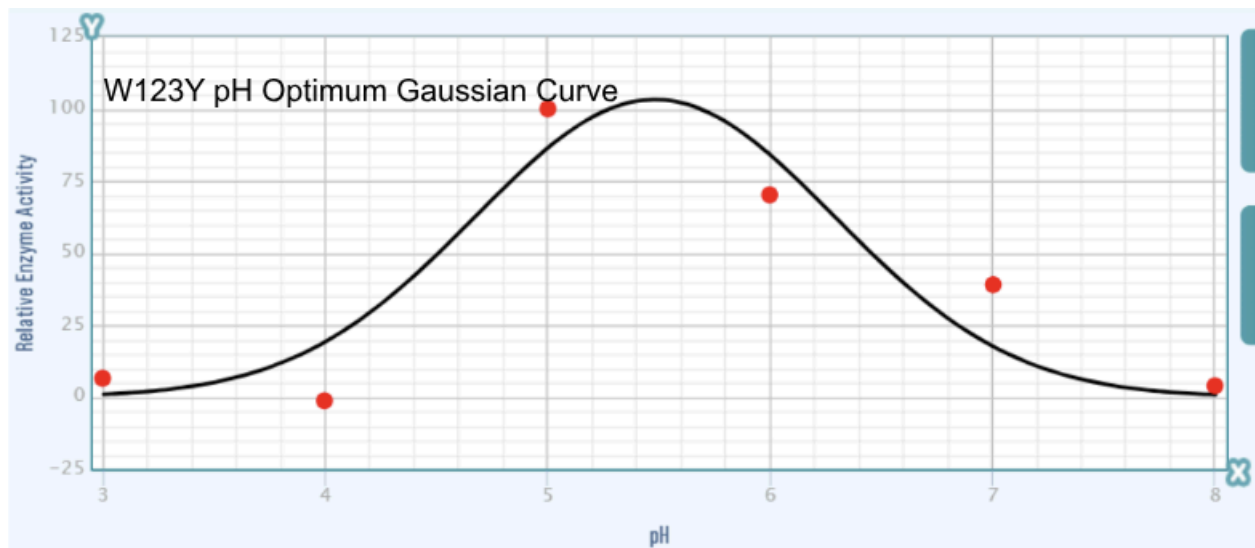


Figure 15, W123Y pH Optimum Gaussian Curve: Relative Enzyme Activity graphed against pH. Used to determine the optimal pH.

Figures 14 and 15 show the optimal pH for BglB to be pH 6.5 and pH 5.5 for WT and variant respectively, based on the peak of the distribution curve, corresponding to the highest absorbance values. The absorbance values for W123Y BglB were very small relative to the WT.

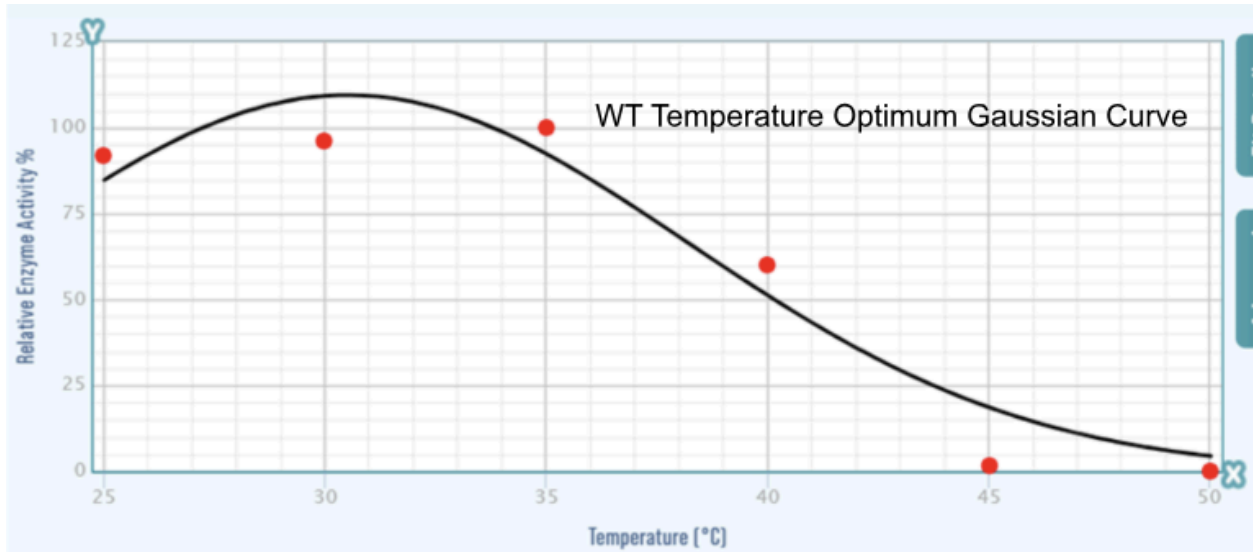


Figure 16, WT Temperature Optimum Gaussian Curve: Relative Enzyme Activity graphed against Temperature in degrees Celsius. Used to determine the optimal Temperature.

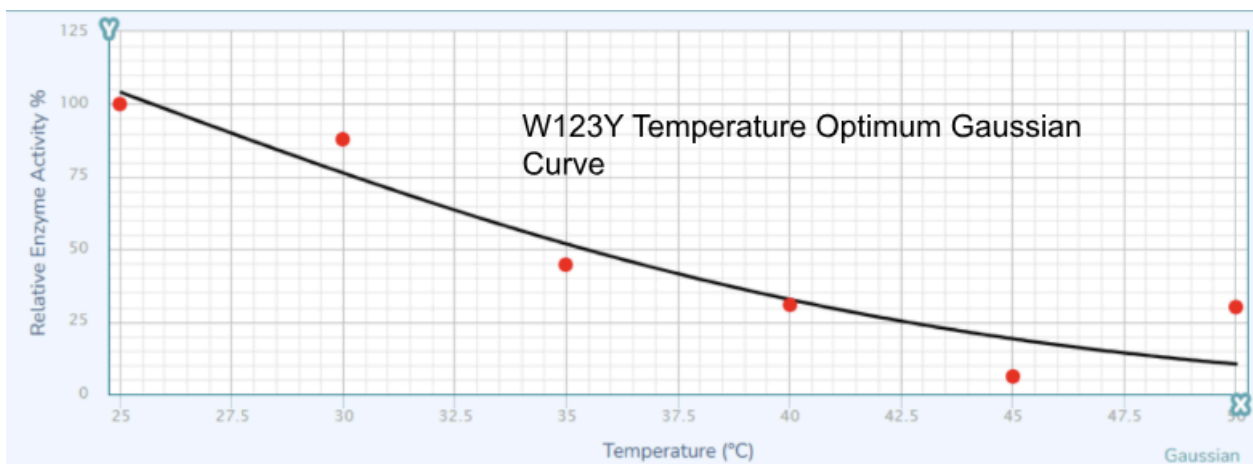


Figure 17, W123Y Temperature Optimum Gaussian Curve: Relative Enzyme Activity graphed against Temperature in degrees Celsius. Used to determine the optimal Temperature.

Figures 16 and 17 show the optimal temperature for BglB to be 30°C and 25°C for WT and variant respectively, based on the peak of the distribution curve, corresponding to the highest absorbance values. The absorbance values for W123Y BglB were very small relative to the WT.

Discussion

This study aimed to analyze the effect of an amino acid substitution on the BglB enzyme through a three part, ground-up workflow. The three parts bridged plasmid engineering, protein expression, and functional analysis, enabling direct investigation of structure function relationships. Overall, the results suggest the W123Y substitution has a significant, deleterious effect on BglB's enzymatic activity, demonstrating the substantial impact a conserved, non-catalytic mutation can have on enzymatic function.

In part 1, the W123Y plasmid was engineered via site-directed mutagenesis. By amplifying the mutant plasmid and sequencing, successful incorporation of the mutation was confirmed. The initially isolated WT plasmid was electrophoresed, resulting in a linear band at the same approximate size of the plasmid, supporting successful isolation. Further diagnostic restriction digestion gel results support the presence of the BglB gene within the plasmid. After site-directed mutagenesis, the mutant amplified plasmid is expected to be linear and at a high concentration, which is corroborated by the post-SDM gel. Following processing and further amplification, the mutant plasmid was electrophoresed, resulting in bands supporting successful isolation. The presence of the specific substitution was confirmed by sequencing before proceeding. The results were of high quality and indicated clear, overlapping readings between the forward and reverse primers. The sequences indicated a single TGG (W) → TAT (Y) substitution for both plasmid samples, with no other significant differences within the reliable range, indicating mutagenesis was successful.

In part 2, W123Y BglB protein was induced and isolated by bacterial transformation, IPTG induction, and affinity chromatography. By conducting SDS-PAGE and Western Blot, successful protein expression and purification was confirmed. Following column chromatography, samples were separated by size via SDS-PAGE and stained, showing the presence of a ~50 kDa band across post induction-elution samples, corresponding to BglB's size. This indicates successful protein expression, and in the final elution samples, this band is mostly isolated, suggesting a relatively pure isolation. Another set of gel samples underwent Western Blot, where precipitate formed along this ~50 kDa band, confirming the presence of the 6xHis tagged protein. Together, the elution samples were determined to contain BglB protein with relative purity.

In part 3, the functional effect of the W123Y mutation was evaluated using computational modeling and enzymatic activity assays. Using Foldit, the W123Y mutation was introduced, yielding a Δ TSE of +20.379, which predicts significant destabilization and suggests a loss of enzymatic activity. The enzyme activity of the purified W123Y BglB protein was analyzed in-gel, and visually no substrate fluorescence was discernible in the gel. Further processing showed normalized activity below 10% for all mutant samples, indicating very little activity relative to the WT BglB. Conducting the kinetic activity assay revealed a nearly flat Michaelis-Menten Curve with V_{max} and K_m values near zero. As such, the calculated k_{cat} and catalytic efficiency values are very small, indicating very little catalytic activity. These experimental results are consistent with the Foldit prediction, suggesting the residue W123 plays an important role in substrate positioning or maintaining active site structures. Substitution to tyrosine introduces polarity and may disrupt residue-substrate interactions or packing, leading to decreased stability and catalytic efficiency.

In line with the previous results, the endpoint temperature and pH optimum assays resulted in very small absorbance values for mutant BglB relative to WT. The optimal temperature and pH for BglB was calculated, showing the mutated protein functioned better at lower temperatures and pH compared to the WT protein. These results indicate a decrease in thermal stability and pH resistance and are expected given the Foldit prediction.

Overall, the results are consistent with the expectation that mutations around structurally important regions will influence enzyme activity and stability. As proteins evolved over evolutionary time, it is expected that proteins are mostly optimized and the vast majority of mutations will be deleterious. This is reflected in the very poor activity of the W123Y BglB protein. Due to this, assays that involve enzyme activity, will record values close to background, potentially affecting the results. Additionally, assays that work with very small volumes, such as SDM, incur the risk of pipetting error.

The three-part experimental workflow effectively achieved the objectives of the study, providing a controlled and systematic approach to investigating the effects of the W123Y mutation. This multi-step design allowed for flexibility in experimental timing while maintaining consistency across procedures. Additionally, the workflow is readily adaptable for testing other hypotheses, including different genes or mutations. The use of widely established biochemical techniques enhances reproducibility and reduces overall experimental cost.

Several techniques used in this study have limitations that may have affected data quality and interpretation. The 1% agarose gel electrophoresis used for size separation showed reduced resolution at high DNA concentrations, resulting in band smearing and clumping. Spectrophotometric measurements were dependent on sample purity and could not distinguish between DNA and contaminants that absorb at similar wavelengths, such as residual RNA. Additionally, kinetic measurements relied on manual mixing, introducing variability in the exact reaction start time and potentially affecting initial rate calculations. Sanger sequencing accuracy was limited to approximately 40–800 base pairs and is susceptible to artifacts, restricting sequence verification. Finally, the experimental workflow did not directly measure protein stability, instead relying on indirect assessments through computational modeling and functional assays. Repeating the experiment, improvements could be made by diluting concentrated gel samples, optimizing purification conditions, performing multiple kinetic trials, and incorporating additional assays such as differential scanning fluorimetry to directly measure protein stability (Niesen et al., 2007).

Given these findings, it is logical to consider the effect of other mutations at the same position, both conserved and non-conserved. Would different substitutions result in greater changes in activity or stability? Could smaller residues allow for larger substrate docking? How might multiple targeted mutations affect protein function? Additional experiments following the same workflow could address these questions, perhaps aiming to find a BglB variant with enhanced activity or stability.

In conclusion, this study demonstrates the deleterious effect of the W123Y mutation on BglB function, showing that site-directed mutagenesis coupled with protein expression and functional assays is an effective strategy for exploring enzyme structure function relationships. This study highlights the broader utility of protein engineering in understanding and optimizing enzyme function.

References

- 1.) Bhatia Y, Mishra S, Bisaria VS. *Microbial beta-glucosidases: cloning, properties, and applications. Crit Rev Biotechnol.* 2002;22(4):375-407. PMID: 12487426.
- 2.) Wierenga RK. *The TIM-barrel fold: a versatile framework for efficient enzymes. FEBS Lett.* 2001 Mar 16;492(3):193-8. doi: 10.1016/s0014-5793(01)02236-0. PMID: 11257493.
- 3.) Niesen FH, Berglund H, Vedadi M. *The use of differential scanning fluorimetry to detect ligand interactions that promote protein stability. Nat Protoc.* 2007;2(9):2212-21. doi: 10.1038/nprot.2007.321. PMID: 17853878.